Properties of Sea Water and Its Concentrates Up To 200°C

United States Department of the Interior

Properties of Sea Water and Its Concentrates Up To 200°C

By L. A. Bromley, University of California at San Diego, La Jolla, California, for Office of Saline Water; W. Sherman Gillam, Assistant Director, Research; Francis H. Coley, Chief, Materials Division

Created in 1849, the Department of the Interior--
America's Department of Natural Resources--is concerned with
the management, conservation, and development of the Nation's
water, wildlife, mineral, forest, and park and recreational
resources. It also has major responsibilities for Indian and
Territorial affairs.

As the Nation's principal conservation agency, the
Department of the Interior works to assure that nonrenewable
resources are developed and used wisely, that park and recrea-
tional resources are conserved for the future, and that renew-
able resources make their full contribution to the progress,
prosperity, and security of the United States--now and in the
future.

FOREWORD

This is the two hundred and twenty-seventh of a series
of reports designed to present accounts of progress in saline water
conversion with the expectation that the exchange of such data will
contribute to the long-range development of economical processes
applicable to large-scale, low-cost demineralization of sea or
other saline water.

Except for minor editing, the data herein are as contained
in the reports submitted by the University of California at San Diego
under Contract No. 14-01-0001-363, covering research carried out
through December 31, 1965. The data and conclusions given in this
report are essentially those of the contractor and are not necessarily
endorsed by the Department of the Interior.

SUMMARY

The first phase in a comprehensive study of the physical properties of sea water has been completed. This comprises heat capacity measurements at one atmosphere constant pressure for sea water and its dilutions and concentrates. Ranges covered in this work include salinities from 1.1-11.7% and temperatures from 2 to 80°C. This concentration range is equivalent to about 1/3 to 3½ times the natural concentration of sea water from La Jolla, California. The second phase, heat capacity measurements up to 200°C, has progressed through most of the difficult steps of designing and fabricating the pressure equipment. Fabrication is being completed, and the experiments at elevated temperatures will proceed under the current OSW Research Grant No. 14-01-0001-763, which also includes studies of other properties.

Data for heat capacity as a function of temperature are presented for various salinities in the form of data point plots, least squares linear and quadratic curves, and equations. Equations have been developed for heat capacities of sea water as a combined function of temperature and concentration. A nomograph has been constructed from which heat capacities can be readily estimated to a high degree of accuracy.

Heat capacities obtained for sodium chloride solutions and for a synthetic sea water concentrate are compared with those of sea water solutions at corresponding salinities. Temperature coefficients of heat capacities for salts other than sodium chloride whose ions are present in sea water are compared with those of sea water and sodium chloride solutions.

The development of the design and fabrication of the pressure calorimeter are described.

CONCLUSIONS

1. Heat capacities at one atmosphere constant pressure have been measured for sea water solutions over a concentration range of 1.1-11.7% salinity and a temperature range of 2-80°C. This concentration range extends from about 1/3 to 3½ times that of natural sea water. The accuracy of the results is about 0.1%.

2. These heat capacities as a function of temperature are suitably described by parabolic equations which yield values within one part per thousand of the experimental values. For solutions near the natural concentration of sea water, about 3.36% salinity, the relationship is linear.

3. A nomograph has been constructed from which heat capacities of sea water solutions can be easily estimated to a high degree of accuracy. The nomograph is shown as Figure 28 of the report. It is accurate to within three parts per thousand of experimental values, for 1-12% salinity at 0-80°C and for 0-1% salinity at 10-80°C. In the remaining region of 0-1% salinity from 10° down to 0°, the accuracy drops from three to ten parts per thousand.

4. Equations suited to various degrees of accuracy have been developed for heat capacities of sea water solutions as a combined function of salinity and temperature. In the equations below, C_p is in defined (15°) calories/gram-°C, S is in percent salinity as defined in the report, and T is in °C. The equations are valid for 0-12% salinity at 0-80°C to the indicated accuracies.

     a. Where an accuracy within one percent of experiment is sufficient:

$$C_p = 1.000 - 0.0125S + 0.00020T$$

     b. For an accuracy within five parts per thousand for all conditions except 0-1% salinity at 0-20°C:

$$C_p = 0.9948 - 0.011412S + [(0.42997 + 0.15192S) \times 10^{-4}T]$$

     c. Where extreme accuracy of about one part per thousand is desired:

$$C_p = 1.0049 - 0.016210S + (3.5261 \times 10^{-4}S^2) -$$
$$[(3.2506 - 1.4795S + 0.07765S^2) \times 10^{-4}T] +$$
$$[(3.8013 - 1.2084S + 0.06121S^2) \times 10^{-6}T^2]$$

Exceptions to the stated accuracy for equation "c" are at the two extremes: for salinity of 0% at 0°C, the equation is accurate to within three parts per thousand; at 11.7% salinity at 80°C, within two parts per thousand.

5. Present data show excellent agreement with those of Cox and Smith[1] within their range of -2 to +30°C and 0-4% salinity. Extrapolation of the Cox and Smith equation beyond their experimental limits should not be attempted, as it leads to too high values at higher temperatures.

6. To prepare concentrates higher than that of twice natural sea water, samples must be acidified to a pH of 4.5 to prevent precipitation of $CaCO_3$ and $Mg(OH)_2$.

7. Heat capacities of a sample of sea water obtained at the equator are in excellent agreement with those predicted for that salinity from the equations based on La Jolla

sea water. Samples being obtained from the north Pacific
and from the Atlantic will confirm whether or not the re-
lationships found for La Jolla sea water are valid for
these waters also.

8. Sodium chloride solution heat capacity data were ob-
tained for three concentrations: 3.5, 6.7, and 9.7%S.
Results are in excellent agreement with NaCl solution
data reported in the literature[8, 9, 10].

9. At high concentrations, deviations are apparent be-
tween the temperature dependence of the heat capacities
of sea water and that of corresponding NaCl solutions.
At equal weight percent salinities of 9.7%, heat capa-
cities are approximately the same at 80°, but they show
increasing deviation with decreasing temperature, until
at 25° they differ by about five parts per thousand. The
sea water solution shows the greater change. Conclusions
have not been drawn below 25° because of the limited
amount of data obtained for sodium chloride solutions at
the low temperatures; indications are that the difference
becomes even greater.

10. Heat capacities of a synthetic sea water concentrate
containing Na^+, Cl^-, Mg^{++}, and $SO_4^=$ ions approach those
of sea water solutions more closely than do the NaCl solu-
tions. At 9.5% salinity, the heat capacities of the syn-
thetic solution agree with those of the corresponding sea
water solution within two parts per thousand across the
temperature range of 0-80°.

11. Temperature dependence of heat capacities of salts
other than NaCl whose ions are contained in sea water is
more pronounced than that of NaCl solutions. This devi-
ation is greater at the higher concentrations and temper-
atures. Our limited data are confirmed by other investi-
gators. Eigen and Wicke[10] show that at about 1 Molal
concentration, $\Delta C_{p(80°-10°)}$ is about three times as high
for $MgCl_2$ solution as for NaCl solution. Thus the differ-
ences between sea water and NaCl solutions can be quali-
tatively accounted for by the presence of the other ions.
Additional evidence allowing a quantitative evaluation of
the effects of these ions will be sought in the current
program.

12. A pressure calorimeter has been designed, and fabri-
cation partially completed, for heat capacity measure-
ments up to 200°C. The calorimeter is a dome shaped,
gold plated bomb made of beryllium copper. The heater,
a fiber glass insulated resistance wire encased between
two sections of copper tubing, has a heat output of about
100 watts at 100 volts. Temperature is recorded with a

nickel resistance thermometer-bridge-amplifier system. The timing circuit for measuring the heating period is based on a standard pendulum clock. The energy input is determined by measuring voltage and current during the heating period. An overall accuracy of $\pm 0.1\%$ is expected for these high temperature measurements.

Table of Contents

List of Tables

List of Figures

INTRODUCTION

Reliable data on physical properties of sea water and its concentrates are of immediate importance both in desalination studies and in research investigations into the nature of sea water. Realistic predictions of equipment and energy requirements of conversion processes depend upon accurate information as to the variation of physical properties with temperature, composition, and pressure. Because data on natural sea water are meager, it is common to approximate its behavior by using data on sodium chloride solutions, or, worse, those of pure water. Outside of a narrow range of conditions, such approximations are unjustified, and the effects of ions other than Na^+ and Cl^- must be considered.

The present research program under OSW Research Grant No. 14-01-0001-363 consisted of two phases: (1) heat capacity measurements of sea water and various dilutions and concentrations ranging in salinity from 1.1-11.7%, over a temperature range of 2-80°C, and (2) design and construction of a pressure calorimeter for heat capacity measurements up to 200°C. The high temperature measurements will be obtained under OSW Research Grant No. 14-01-0001-763.

Previously, data on heat capacities of sea water have been available only in the temperature range of -2 to +30°C, up to a salinity of 4.0%.[1]

EXPERIMENTAL METHOD (TEMPERATURE RANGE OF 2-80°C)

The method for determining heat capacities at constant pressure of one atmosphere is that of classic calorimetry. An accurately weighed liquid sample is placed into a calorimeter whose "effective heat capacity" has been determined experimentally. A measured amount of electrical energy is introduced into the filled calorimeter, and the resultant temperature rise is noted. The heat capacity of the unknown sample is calculated from the equation:

$$C_{p(sample)}, \text{ cal/g-°C} = \frac{\frac{(\text{energy input, cal})}{\Delta T} - wC_p}{\text{grams of sample}}$$

Calories are defined calories equal to 4.1840 absolute joules[2], and are for the temperature midway between the initial and final temperatures; T is in °C; ΔT is of the order of 3°C; and wC_p is the "effective heat capacity" of the calorimeter at the temperature of the experiment. wC_p is determined from measurements using pure water. Experimental details are given in the sections below.

Calorimeter Design

Figure 1 is a photograph of the disassembled calorimeter and its accoutrements. The calorimeter comprises a five-liter spherical Dewar flask (1), the narrow neck of which is fitted with a Teflon stopper (2) equipped with holes for stirrer, heater, and two thermometers. The jacket (3) is a twenty-liter pressure cooker adapted with inlet and outlet for circulation of water from a constant temperature bath (4). The cover (5) of the cooker has been modified to enclose the neck of the Dewar and to support a pair of concentric, two-foot glass columns (6), between which the jacket water is circulated to maintain a constant temperature above the calorimeter. The temperature in the bath is controlled by means of a Hallikainen Thermotrol unit (7) comprising a sensing probe and a regulator with a controlling sensitivity of 0.001°C. For low temperature runs, ice water is circulated through a copper coil (8) within the bath, at a rate such that the Thermotrol can maintain the proper control at low temperatures. It was possible to maintain constant temperature as low as 2°C.

The electrical energy is supplied by a 1000 watt heater enclosed in a Vycor sheath (9). The firing (heating) time, calculated to yield a temperature rise of about 3°C, is preset with an automatic timer (10). The energy is recorded as watt-hour meter revolutions (about 25 revolutions) to the nearest 0.002 of a revolution by a Sangamo J-5 rotating standard watt-hour meter (11). Several times during the course of the study the meter was checked against the standard meter at the San Diego Gas and Electric Company; the maximum deviation found was 0.03%, considerably better than the manufacturer's rating of 0.1% accuracy. Since the calorimeter is calibrated with distilled water as the primary standard, reproducibility of readings rather than absolute accuracy is the critical factor. Firing time is also recorded (12), although the time does not enter into the calculations. Incoming line voltage is controlled by a Sola voltage regulator (not shown). An auxiliary heater (13) is introduced into the circuit ahead of the main heater to absorb the initial power surge when the switch is first opened to the line voltage. The auxiliary heater is cut out of the circuit when the main heater is turned on.

Stirring within the calorimeter is effected by a three-blade propeller attached to a 316 stainless steel shaft (14) revolving at 300 RPM controlled by a synchronous motor (15). Primary temperature readings are obtained with a combination of a platinum resistance thermometer (16), Mueller bridge (17), and a Leeds and Northrup null-detector (18). By interpolating the null-detector needle
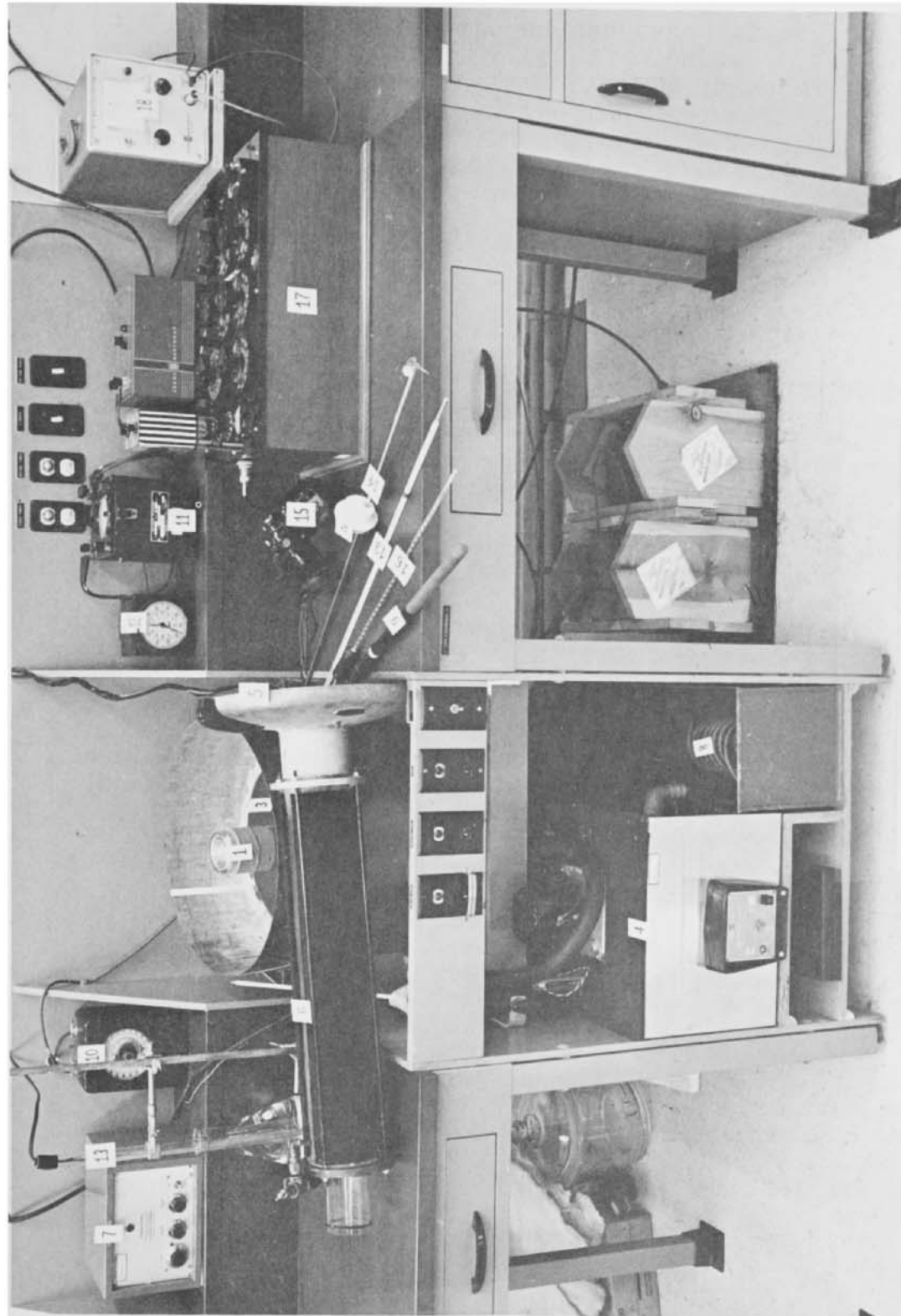
Figure 1

Disassembled Calorimeter

deflection, resistances can be estimated to within $\pm 1 \times 10^{-5}$ ohms, corresponding to $\pm 1 \times 10^{-4}$ °C. A calibrated mercury thermometer (19) is placed in the calorimeter as a secondary indicator when quick, approximate readings of temperature within the calorimeter are desired.

The assembled calorimeter is shown in Figure 2.

Calorimeter Operation

The procedure for determining heat capacities of sea water and its concentrates is as follows:

4330 ± 5 cc of the solution is measured into volumetric containers at about the temperature of the first experiment of each series (e.g., about 2 to 5°C), weighed on a Mettler K-4 balance with an accuracy of ± 0.2 g, and poured into the calorimeter. This volume is such that the water level within the calorimeter fills about one-half the narrow neck of the Dewar after assembly is completed. As each sucessive experiment within a series is run at a higher temperature than the preceding one, water is removed quantitatively between experiments, using a modified burette, so as to keep the liquid level approximately constant throughout the series.

After the water is introduced into the calorimeter, the various parts are assembled. The bath temperature is adjusted to about $1\frac{1}{2}$°C above the temperature within the calorimeter. The system is allowed to stabilize thermally. This requires about two to three hours after assembly, or about one hour where disassembly is not required between runs. Thermal stabilization prior to the heating cycle is indicated by a constant temperature rise with time, due to the heat of stirring and heat transfer with the jacket. The heating cycle consists of introducing electrical energy via the 1000 watt heater immersed into the liquid for a period of about sixty seconds. This results in about a three degree rise in temperature. Thermal equilibrium is reached in twenty or thirty minutes after firing, after which the temperature change closely approximates a linear function with time. Temperature readings are taken at about five minute intervals, until at least $1\frac{1}{2}$ hours after heating. The steepness of slope of temperature vs. time is determined by the amount of heat input due to stirring and the amount of heat gained from, or lost to, the environment. Thus, at low temperatures, the slope is slightly positive or zero; at higher temperatures it becomes increasingly negative as the heat loss to the surroundings exceeds the heat of stirring.

Because the temperature rise is not instantaneous after firing, it is necessary to obtain T_0, the temperature at a hypothetical zero time, t_0, by an indirect method. We
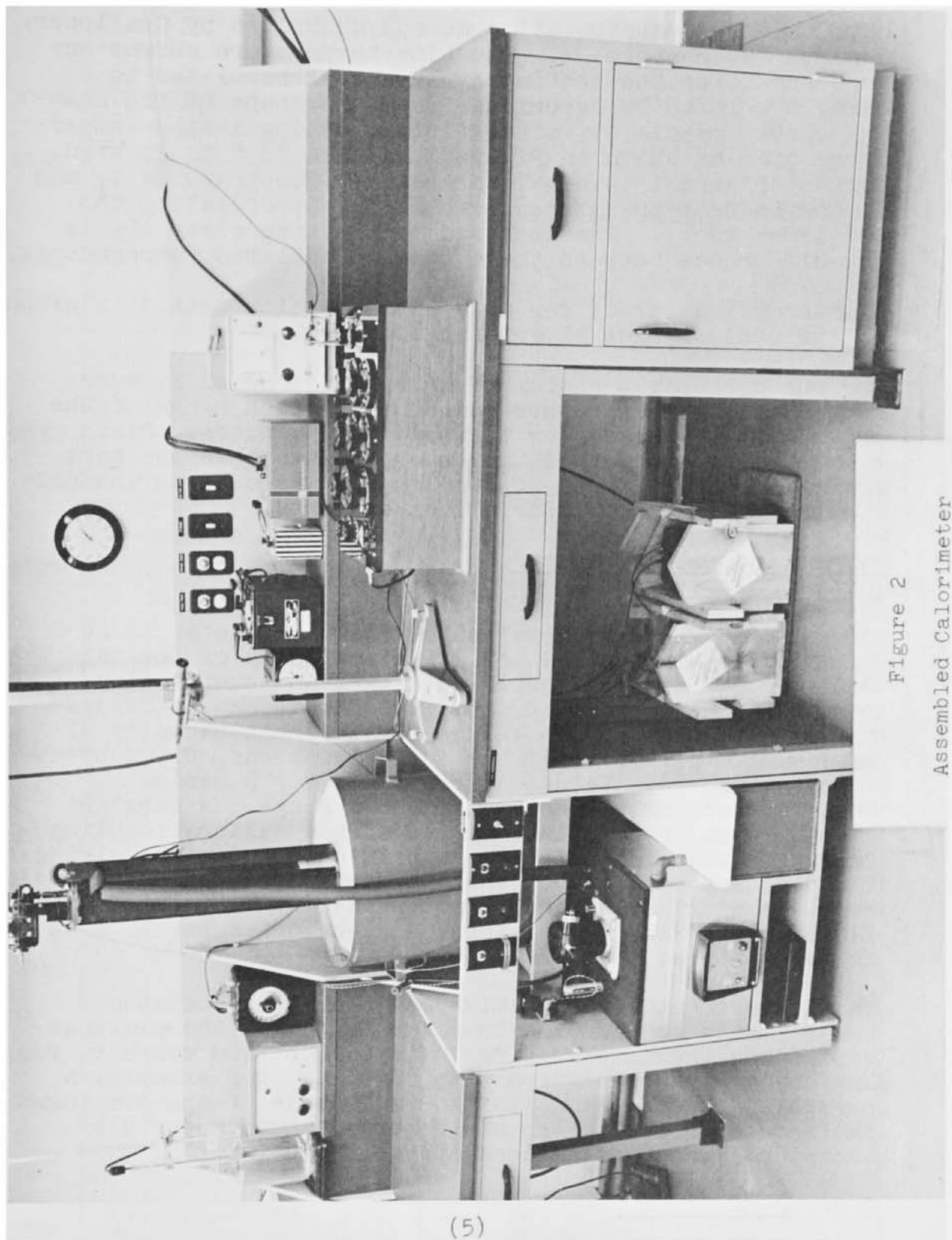
Figure 2

Assembled Calorimeter

have used the extrapolation method described by Challoner, Gundry, and Meetham[3]. The time-temperature curves before and after the heating cycle are extrapolated to a time, t_o, which is determined from the shape of the heating curve immediately after firing. Using a time-temperature plot as shown in Figure 3, a time "t_o" is located for which Area 1 is equal to Area 2. Temperatures T_1 and T_2 are those temperatures reached by extrapolating the two lines to t_o. The required temperature rise, ΔT, is the difference between these two extrapolated temperatures.

A mathematical proof for this extrapolation method is given in the Challoner et al reference.

For our systems, a number of determinations of t_o were made over the temperature and concentration range of the experiments. Values for t_o were $1\frac{3}{4}$-2 minutes. Since even $\frac{1}{2}$ minute results in an error of less than one part per ten thousand, a t_o of two minutes was used in the calculation of T_1 and T_2 for all experiments.

"Effective Heat Capacity" of the Calorimeter

The "effective heat capacity" of the calorimeter is obtained by measuring the total heat capacity of the calorimeter filled with distilled water, and subtracting from this the known heat capacity of that amount of distilled water. Accurate values for the heat capacity of water are available from the work of Osborne, Stimson, and Ginnings[4]. Values are obtained for a series of temperatures across the experimental range. A straight line through these points serves as the calibration line from wich wC_p at any temperature is selected when solving for the heat capacity of unknown samples. The "effective heat capacity" of our calorimeter is of the order of 120-140 calories, increasing about 0.25 calories per °C rise in temperature.

This experimental calibration cancels out systematic errors, such as the time-temperature lag in the platinum resistance thermometer. Periodic calibration corrects for any changes in the system with time, as, for example, a possible gradual change in the resistance of the platinum thermometer. The latter was observed independently by occasional redeterminations of the ice point.

Sources of Error

Systematic errors are avoided by the calibration of the system. Those errors which remain, together with an estimate of their magnitude, are listed in Table 1.

Figure 3 Typical Method of Determining "t_o" by Extrapolation of Time-Temperature Curves.
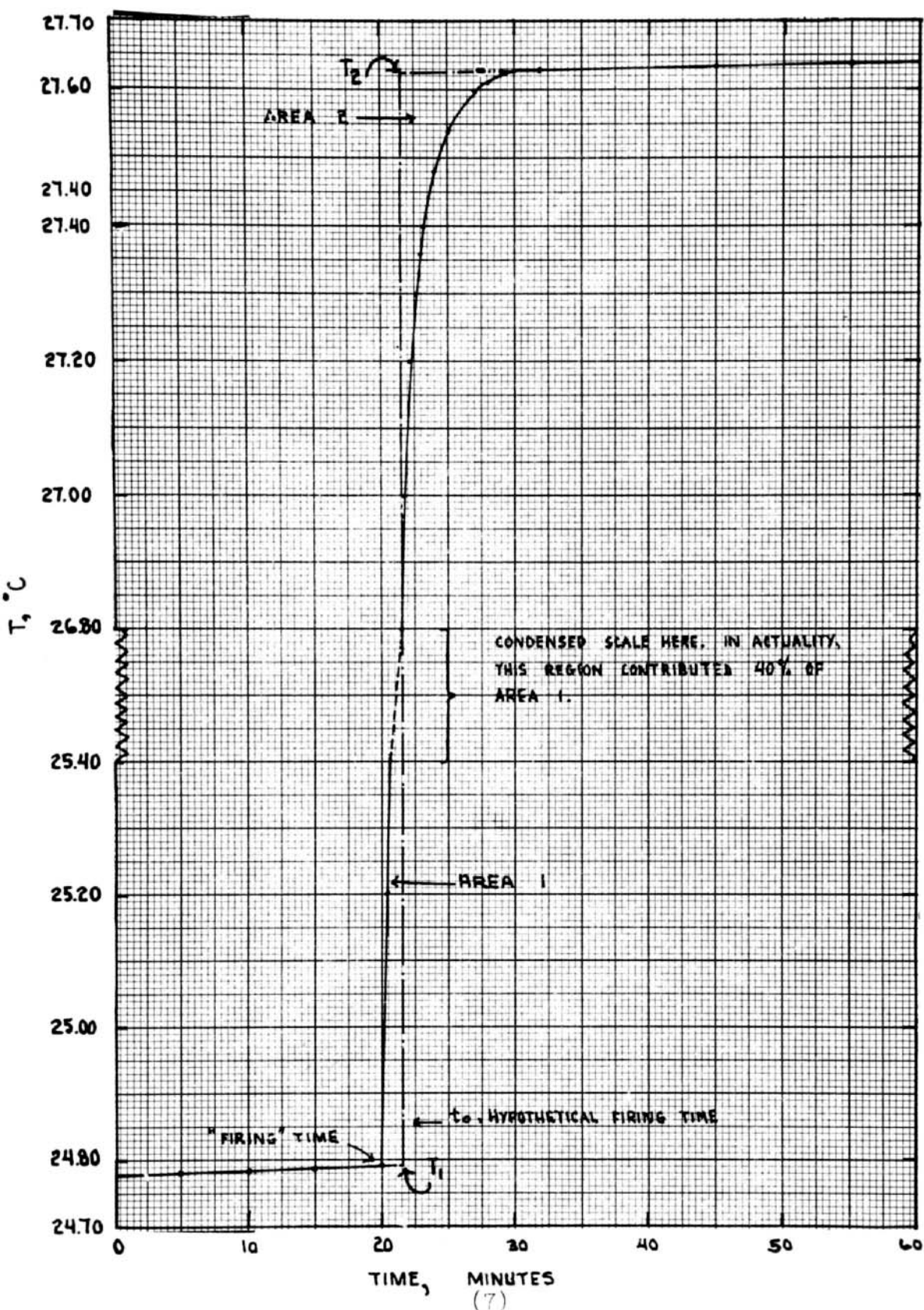
Table 1

POSSIBLE ERRORS IN HEAT CAPACITY MEASUREMENTS

Possible Error	Magnitude	Effect on C_p, %
Calibration uncertainty	2 cal. max.	0.05 max.
Watt-hour meter repro- ducibility		0.03 max.
Extrapolation of T_1, T_2	0.0002°/reading	0.02
Reading T_1, T_2	0.0001°/reading	0.02
Weight of water	0.2 grams/reading	0.02

Assuming errors are additive, an accuracy of 0.14% can be expected. As will be seen from the figures presenting the experimental data, agreement between consecutive runs is certainly this good and generally considerably better.

Materials

Sea Water

Source of Sea Water.--With one exception, all samples of sea water used in this study have been obtained directly from the end of the Scripps pier at La Jolla, California, at a depth of six to ten feet from the bottom of the ocean. Sea water here is relatively free of contaminants and maintains a fairly constant salinity. Typical salinities are shown in Table 2.

Table 2

TYPICAL SALINITIES FOR LA JOLLA SEA WATER[5,6]

	% S
Jan '63 - June '65 minimum monthly mean	3.359
Jan '63 - June '65 maximum monthly mean	3.385
1959 annual mean	3.375
1964 annual mean	3.373

Salinities in the La Jolla region are roughly half-way between those of the northern and southern extremities of the California and Baja California coast. Values for three locations along this coast are shown in Table 3.

Table 3

SALINITIES OF SEA WATER ALONG THE CALIFORNIA COAST[6]
(1964 values obtained on CCOFI* cruise 6401)

	%S
La Jolla	3.373
San Francisco	3.275
Baja Calif., lower tip	3.450

*California Cooperative Oceanic Fisheries Investigations

Thus, the La Jolla waters may be considered as "average" or "typical" California coastal sea waters.

It was of interest to ascertain that results obtained for La Jolla water could be generalized for all Pacific waters. For this reason, a sample of water was obtained from the equatorial Pacific by the Scripps research vessel Agassiz. Another sample is now being obtained from the Aleutian Islands region, and will be analyzed when received.

Because changes, primarily biological, occur in sea water on standing, every effort is made to initiate heat capacity measurements soon after the samples are drawn. After filtering through coarse filter paper, or otherwise treating the sample as will be described in the next section, the sample is chilled over-night. Heat capacity experiments are begun the next day.

Treatment of Sea Water.--Sea water at its normal concentration was treated by one of two methods: (1) filtering through a coarse filter paper, or (2) filtering through diatomaceous earth, acidifying to a pH of about 4.5 with concentrated sulfuric acid, and then degassing. This second procedure is typical of what is followed in evaporation desalination units, where acidification near a pH of 4.5 assures that $CaCO_3$ or $Mg(OH)_2$ precipitation will not occur even in sea water concentrated to more than three times its normal concentration. Degassing is accomplished in a large-scale unit by spraying into air to remove CO_2, then passing through a vacuum deaerator to remove remaining dissolved gases. The unit, which is part of a project supported by the University of California Water Resources Center, is shown in Figure 4. The final pH of the sea water is between 5 and 6. As will be noted later, the acidification and deaeration do not significantly change the heat capacity.

Concentration and Dilution of Sea Water.--Sea water concentrates are obtained by a careful evaporation of water until the desired concentrate is reached, as cal-

Figure 4

Unit for Degassing Sea Water
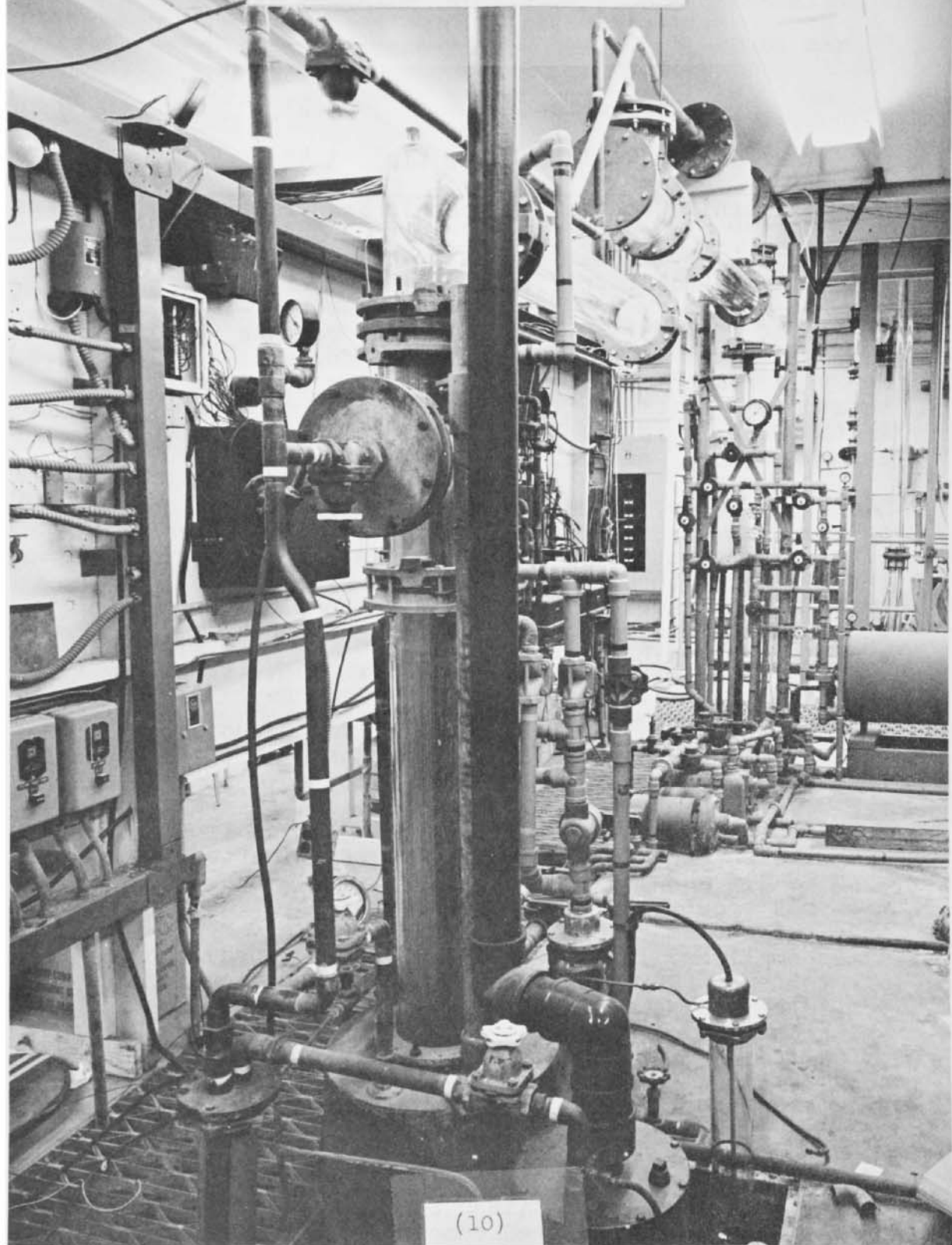
culated by weight loss. In all cases, the calculated weight loss resulted in exactly the salinity expected, indicating at least that no halides have been lost through evaporation. Furthermore, as mentioned above, no precipitation occurred during evaporation. We have therefore been assured that no significant change in the relative composition of the ions has occurred by concentrating the sea water.

Concentrates of $1\frac{1}{2}$, 2, $2\frac{1}{2}$, 3, and $3\frac{1}{2}$ times normal sea water salinity were prepared.

Dilutions of sea water were prepared by addition of the appropriate amounts of distilled water. Dilutions of 2/3, 1/2, and 1/3 normal sea water concentration were prepared.

Sodium Chloride Solutions

Sodium chloride solutions at concentrations approximately those of 1, 2, and 3 times normal sea water concentration were prepared from distilled water and reagent grade NaCl.

Synthetic Sea Water

A synthetic sea water was prepared in which the total number of ions per kilogram of water were the same as are present in triply concentrated La Jolla sea water. In the synthetic water, Na^+ was substituted for all monovalent positive ions; Mg^{++} or Ca^{++} for all divalent positive ions; Cl^- and $SO_4^=$ for mono- and divalent negative ions, respectively. Such a solution is equivalent to sea water in the number of ions, ionic equivalents, and ionic strength, but not in weight percent. The synthetic sea water contains 9.53% solids; the salinity of a triply concentrated La Jolla sea water is 10.1%.

Analysis for "Salinity"

"Salinity" is a defined term and, for sea water, is slightly lower (about 4 parts per thousand) than the total dissolved solids. It is determined by an indirect method of titrating halides with $AgNO_3$, as will be explained. The definition of salinity, established by an International Commission for the production of a "Standard sea water" in 1902, is "the total amount of solid material, in grams, contained in one kilogram of sea water when all the carbonate has been converted to oxide, the bromine and iodine replaced by chlorine, and all organic material completely oxidized"[7]. It has been observed by oceanographers that, in general, except near the mouths of rivers, the relative propor-

tions of the various ions in sea water remain constant,
regardless of the total concentration. Thus, it is
possible to analyze for a major constituent, and from
it determine the salinity.

The analysis for halides by titration with standard
$AgNO_3$ solution, using a K_2CrO_4 indicator is a simple
and accurate one, and, consequently, is a standard
method for determining salinity. The "chloride equi-
valent" is "the total amount of chlorine, bromine, and
iodine in grams per kilogram of sea water, assuming
the bromine and iodine had been replaced by chlorine".
"Chlorinity" is also a defined term, and is equal to
chloride equivalent divided by 1.00045, due to changes
in atomic weights since the time when "primary standard
sea waters" were established by the International Com-
mission. The entire subject of chlorinity and salinity
is largely empirical, and, rather than present a detail-
ed discussion here, we refer the reader to reference 7,
pp. 50 et seq.

Salinity is determined from chlorinity by means of the
following relationship:

$$S = 0.03 + 1.805 \text{ Cl}$$

In the above equation, "salinity" and "chlorinity" are
in parts per thousand. In this report, the more fa-
miliar unit of % is used.

EXPERIMENTAL RESULTS (TEMPERATURE RANGE OF 2-80°C)

The experimental heat capacities as a function of temp-
erature are shown in the figures to follow. All heat
capacities are expressed in units of defined (15°) cal-
ories/gram-°C. One calorie equals 4.1840 absolute joules.

In most cases, at least two series were run in the same
region of concentration. At concentrations of special
interest, such as natural sea water and highly concen-
trated sea water, additional series were run. A few
series run during the latter weeks of the program were
not duplicated if the results of the first series were
in very good agreement with the values calculated from
the Cp versus salinity equations developed by that time.
The type of sample pretreatment is indicated on each
figure.

Figure 5 shows the smoothed curve for the heat capacit-
ies of distilled water, taken from the data of Osborne,
Stimson, and Ginnings[4]. Figures 6-20 present data on
sea water solutions; Figures 21-23, NaCl solutions; and

Figure 5 Heat Capacities of Distilled Water
(Data from Osborne, Stimson, and Ginnings(4))

(13)
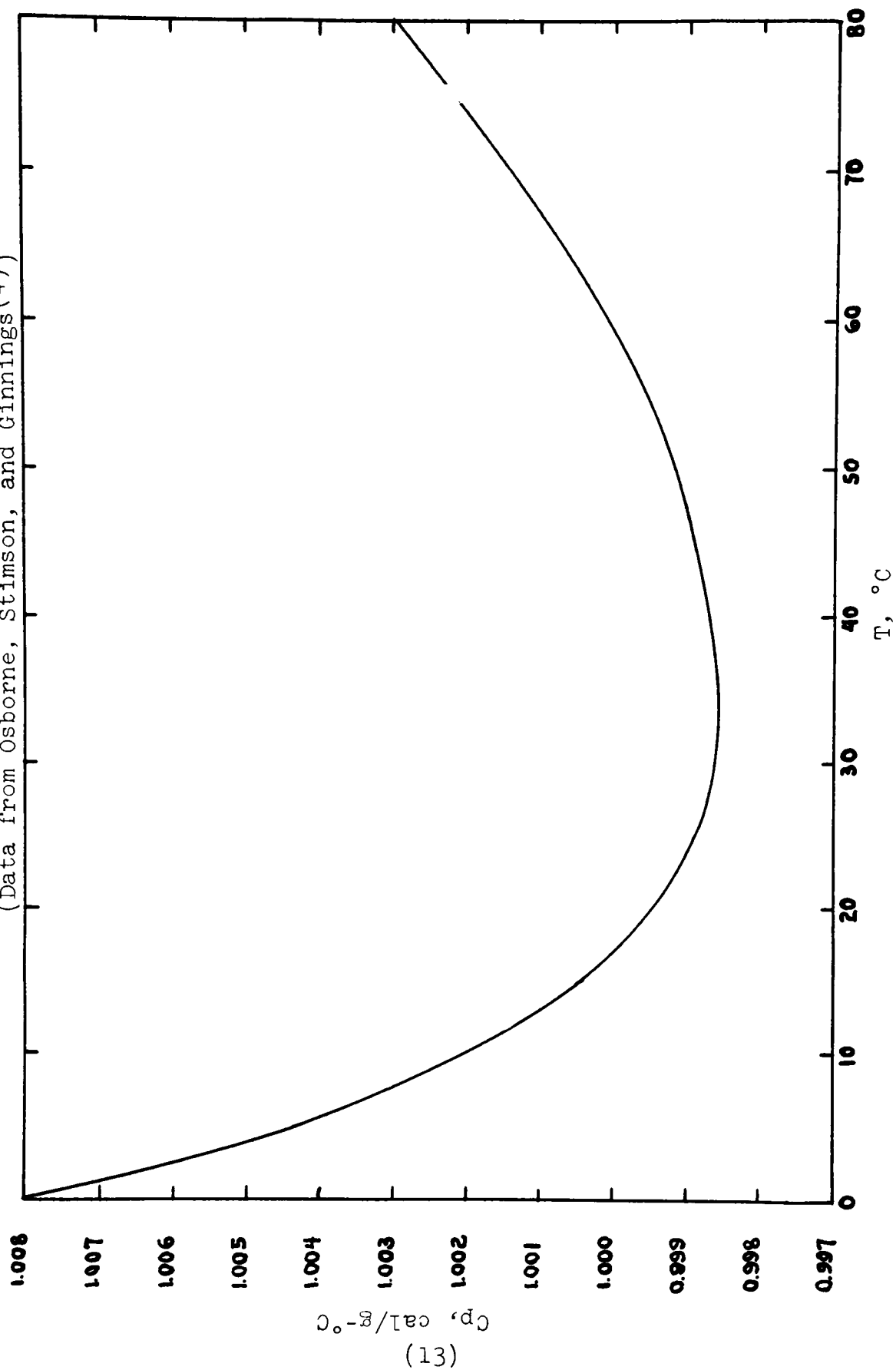
Figures 24-25, solutions of other electrolytes. The ex-
perimental points are indicated by ⊙; where additional
points have been added from other references for compar-
ison, they are so indicated in the legend. Each figure
contains two curves --a straight line and a quadratic
curve. These are the least squares curves obtained for
the data points by computer programming. A double pre-
cision least squares curve fitting program was used with
a Control Data Corporation 3600 computer.

Sea Water Solutions (Figures 6-20)

The figures on the following pages for heat capacities
of sea water solutions are arranged in order of increas-
ing salinity --from 1.12%, approximately one-third that
of La Jolla sea water, to 11.7%, approximately three and
one-half times that of sea water. It may be seen that
the decidedly parabolic curve, convex to the temperature
axis, for distilled water becomes increasingly more nearly
linear as natural sea water concentration is approached,
and slightly concave to the temperature axis as concentra-
tion is increased further. This is illustrated further
in Table 4, which lists the standard deviations for both
types of equations for each concentration.

<p align="center">Table 4</p>

STANDARD DEVIATIONS FOR LINEAR AND QUADRATIC EQUATIONS OF HEAT CAPACITY AS A FUNCTION OF TEMPERATURE

Salinity, Wt. %	Standard Deviation, σ, x 10^4		$\sigma_{Quad}/\sigma_{Linear}$
	Linear Eq.	Quadratic Eq.	
1.12	10.8	3.1	.28
1.65	12.8	4.5	.34
1.69	8.8	2.7	.31
1.70	7.6	3.8	.50
2.23	6.0	2.9	.48
3.00	4.1	2.4	.59
3.36*	6.8	6.3	.93
3.40	5.5	4.7	.85
5.01	6.4	3.0	.47
6.68	9.6	5.6	.58
8.32	10.4	4.0	.38
9.53 (synth.)	10.4	5.5	.55
9.96	7.2	4.4	.61
10.10	13.9	9.5	.68
11.4	14.2	5.5	.39
11.74	11.6	6.9	.59

* Several samples, ranging from 3.34 to 3.38% S.

Figure 6 Heat Capacities of Dilute La Jolla Sea Water at 1.12% Salinity.
(Approximately 1/3 natural concentration)
Two series. Each sample filtered through coarse filter paper.

1 $C_p = 0.9844 + 4.4645 \times 10^{-5} T$ $\sigma = 1.08 \times 10^{-3}$

2 $C_p = 0.9872 - 1.5295 \times 10^{-4} T + 2.3553 \times 10^{-6} T^2$ $\sigma = 3.1 \times 10^{-4}$
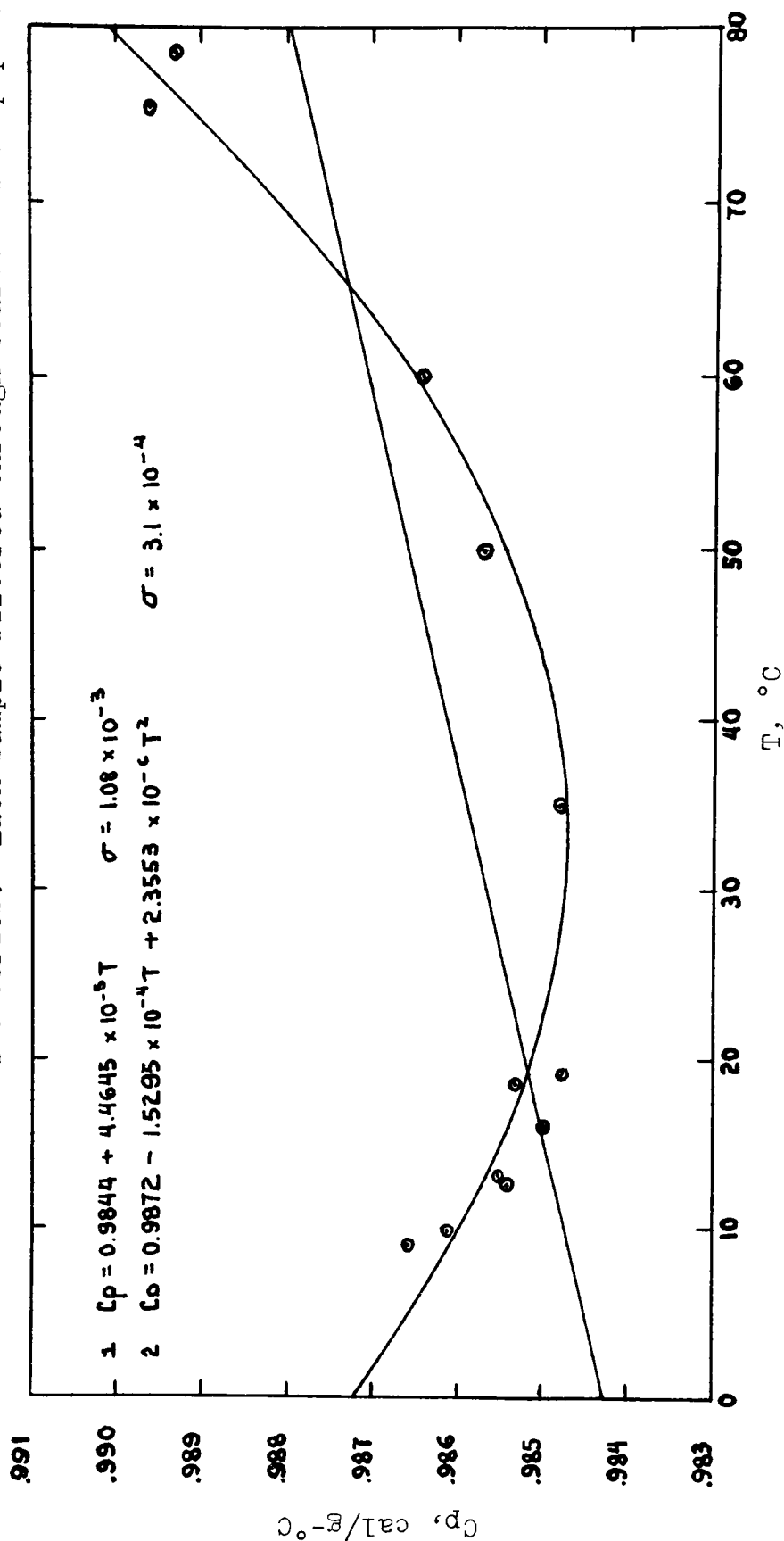
Figure 7 Heat Capacities of Dilute La Jolla Sea Water at 1.65% Salinity. (Approximately 1/2 natural concentration) One series. Filtered through coarse filter paper.

1 $C_P = 0.9763 + 6.758 \times 10^{-5} T$ $\sigma = 1.3 \times 10^{-3}$

2 $C_P = 0.9793 - 1.2071 \times 10^{-4} T + 2.0986 \times 10^{-6} T^2$ $\sigma = 4.5 \times 10^{-4}$

(91)
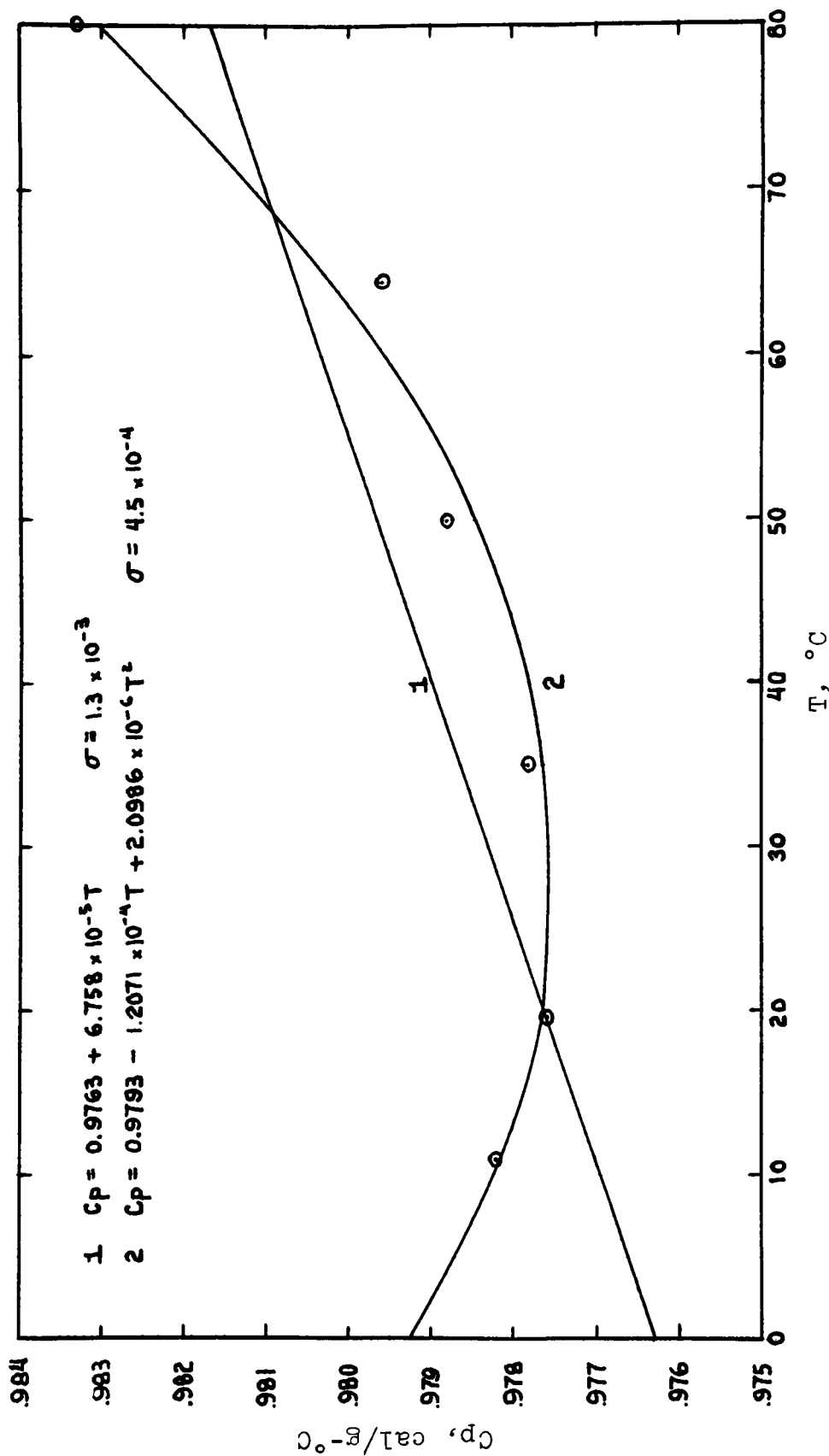
Figure 8   Heat Capacities of Dilute La Jolla Sea Water at 1.69% Salinity
(Approximately 1/2 natural concentration)
Two Series.   Filtered through coarse filter paper.

1. $C_p = 0.9764 + 5.4852 \times 10^{-5} T$ $\sigma = 8.8 \times 10^{-4}$

2. $C_p = 0.9782 - 8.625 \times 10^{-5} T + 1.8148 \times 10^{-6} T^2$ $\sigma = 2.7 \times 10^{-4}$

(17)
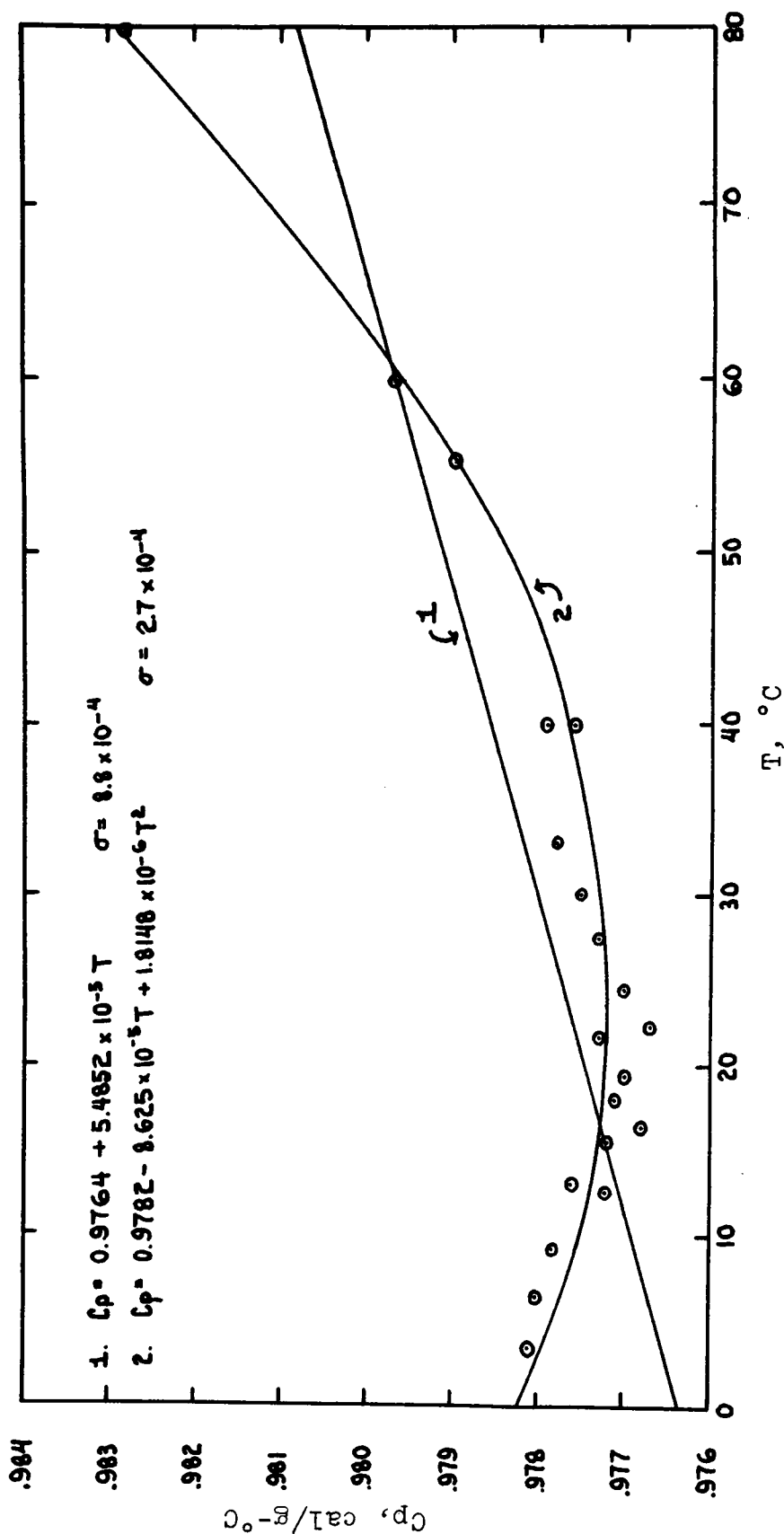
Figure 9 Heat Capacities of Dilute La Jolla Sea Water at 1.70% Salinity. (Approximately 1/2 natural concentration) Two series. Filtered through coarse filter paper.

1 $c_p = 0.9759 + 5.0519 \times 10^{-5} T$ $\qquad \sigma = 7.6 \times 10^{-4}$

2 $c_p = 0.9776 - 8.9068 \times 10^{-5} T + 1.8249 \times 10^{-6} T^2$ $\qquad \sigma = 3.8 \times 10^{-4}$

(18)
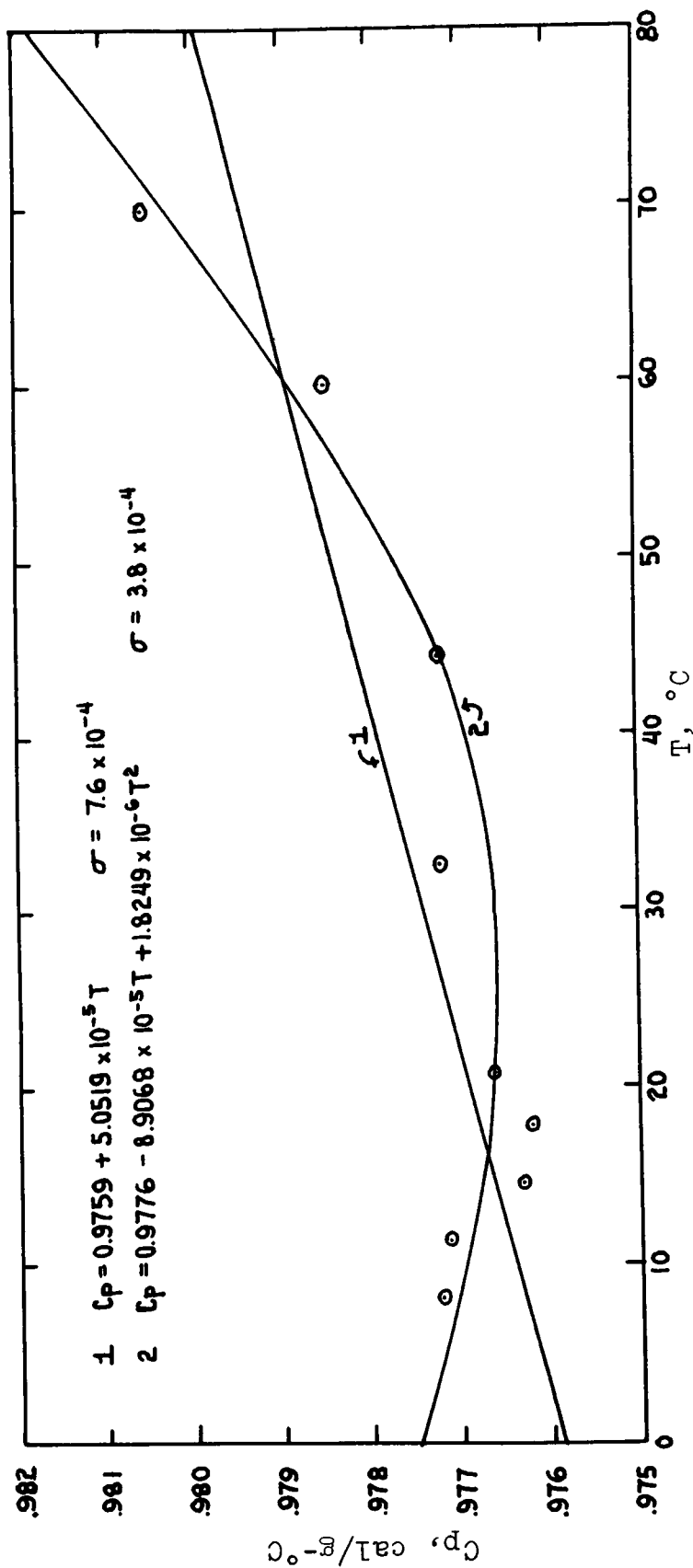
Figure 10   Heat Capacities of Dilute La Jolla Sea Water at 2.23% Salinity
(Approximately 2/3 natural concentration)
One series. Filtered through coarse filter paper.

1   $C_p = 0.9687 + 8.604 \times 10^{-5} T$ $\sigma = 6.0 \times 10^{-4}$

2   $C_p = 0.9700 - 5.175 \times 10^{-6} T + 1.0614 \times 10^{-6} T^2$ $\sigma = 2.9 \times 10^{-4}$

$\triangle$ CALC. FROM COX AND SMITH EQUATION

C_p, cal/g-°C

T, °C

(61)
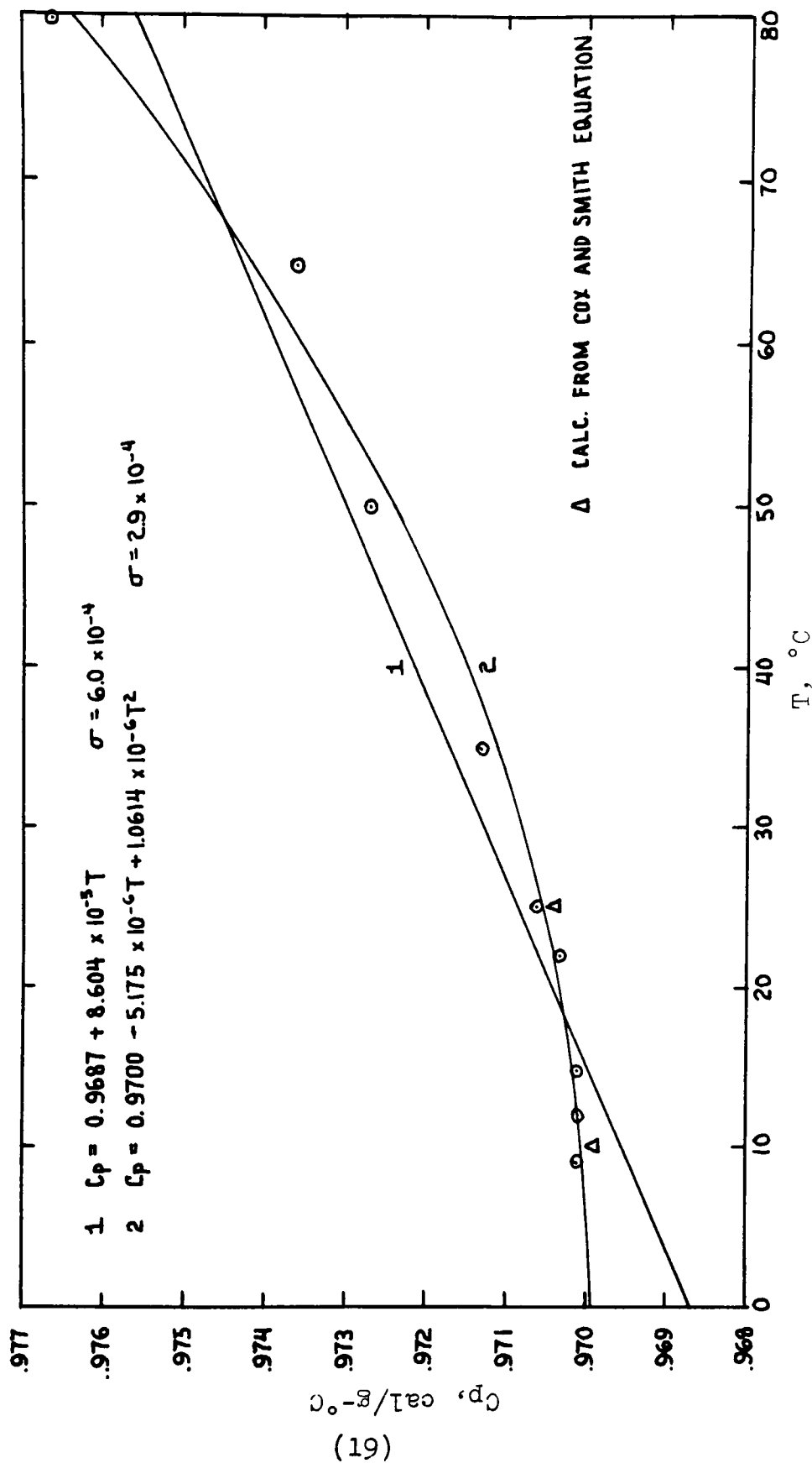
Figure 11 Heat Capacities of Dilute La Jolla Sea Water at 3.00% Salinity.
(Approximately 0.9 natural concentration)
One series. Filtered through coarse filter paper.

1 $C_p = 0.9579 + 1.1410 \times 10^{-4} T$ $\sigma = 4.1 \times 10^{-4}$

2 $C_p = 0.9583 + 5950 \times 10^{-5} T + 8.158 \times 10^{-7} T^2$ $\sigma = 2.4 \times 10^{-4}$

$\triangle$ COX AND SMITH EXPERIMENTAL VALUES

—— CURVE OBTAINED WITH COX AND SMITH EQUATION, EXTENDED BEYOND THEIR UPPER LIMIT OF 30°C.

C_p, cal/g-°C

T, °C

(20)
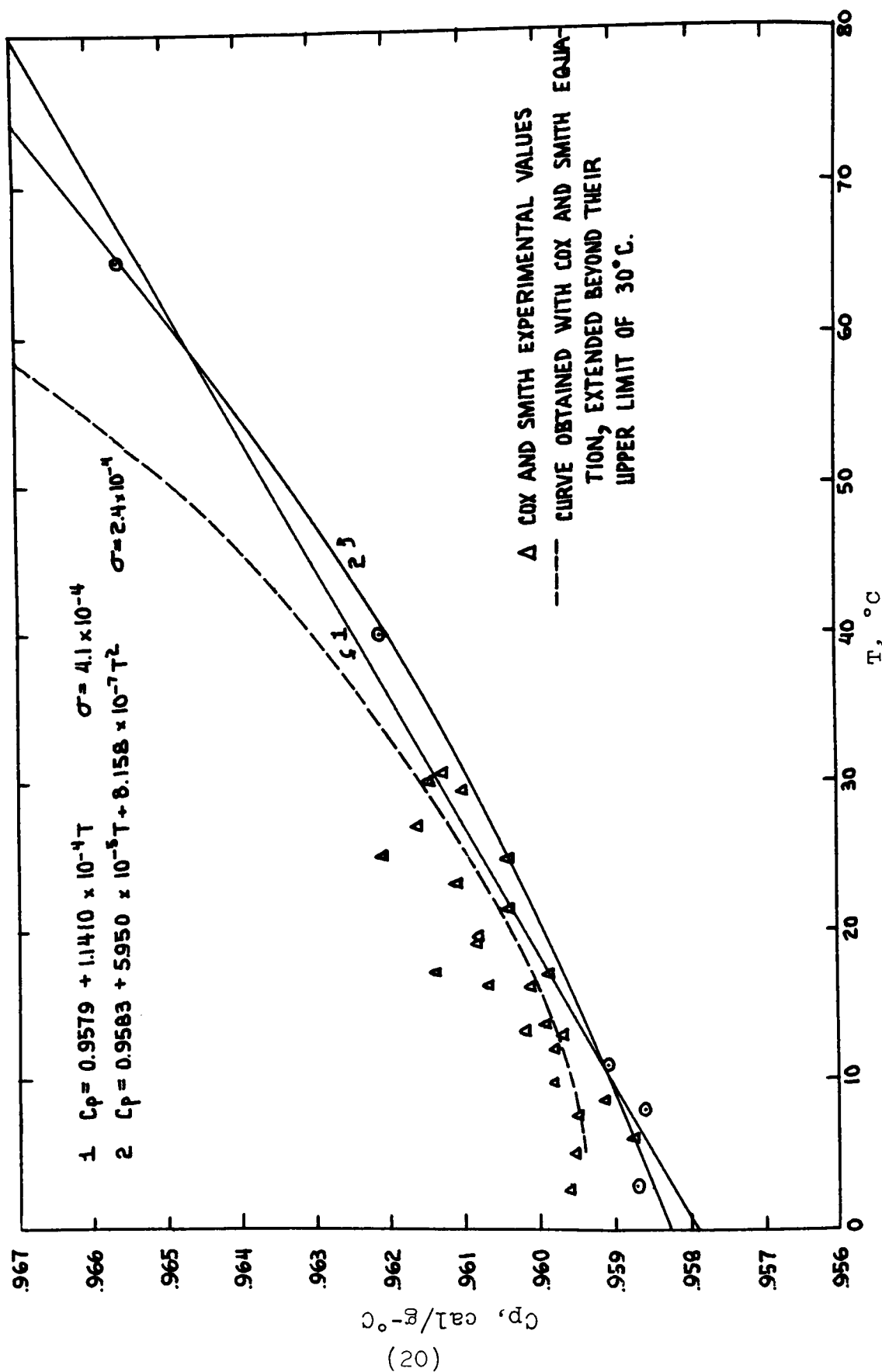
Figure 12 Heat Capacities of La Jolla Sea Water at 3.34 – 3.38% Salinity. (Natural concentration) Seven series. Five filtered through coarse filter paper. Two filtered through diatomaceous earth, acidified to 4.5 pH, and deaerated to ~6.0 pH.

1 $C_P = 0.9546 + 1.1349 \times 10^{-4} T$ $\sigma = 6.8 \times 10^{-4}$

2 $C_P = 0.9553 + 6.381 \times 10^{-5} T + 5.605 \times 10^{-7} T^2$ $\sigma = 6.3 \times 10^{-4}$

(21)
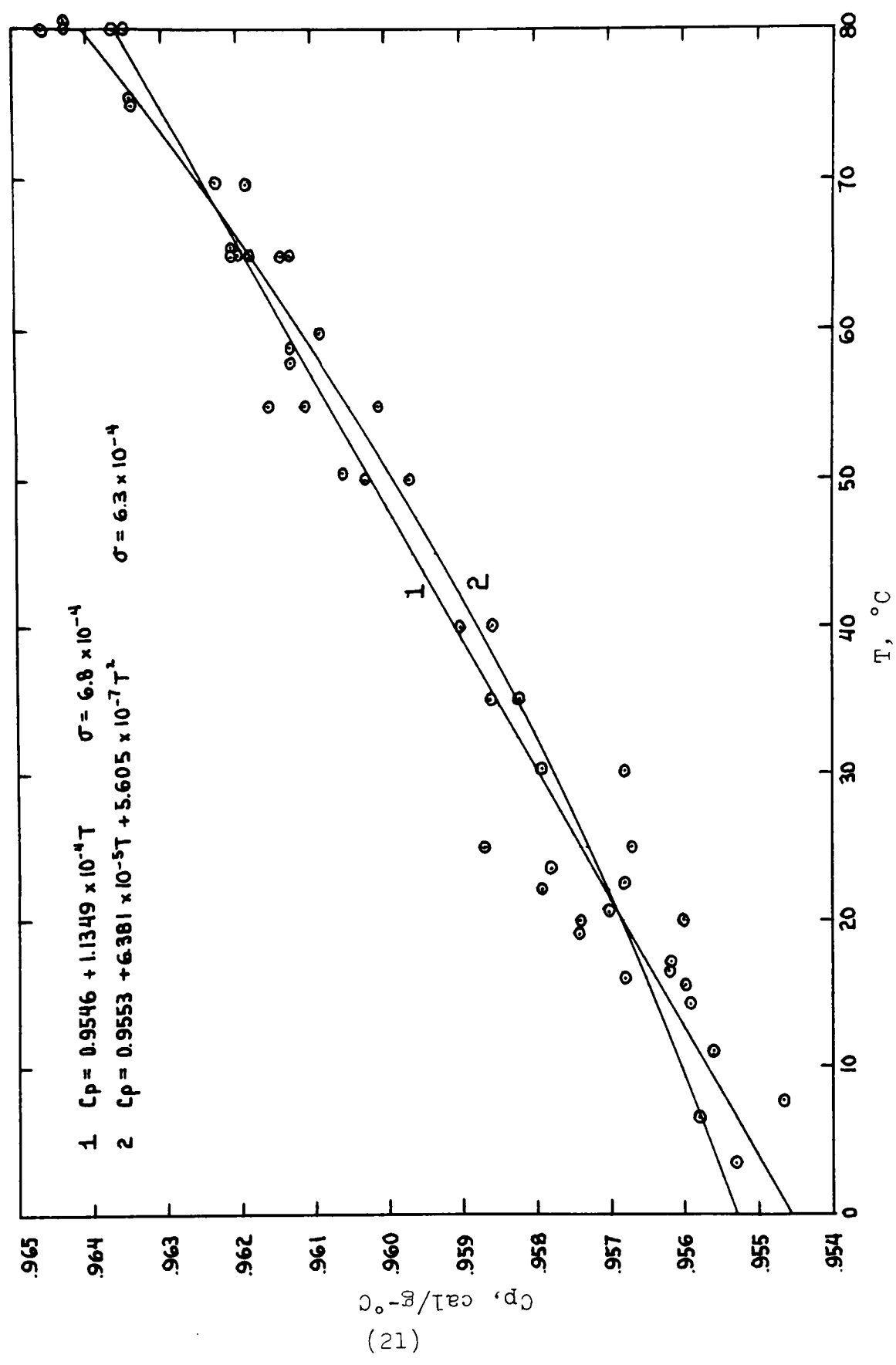
Figure 13 Heat Capacities of Equatorial Sea Water at 3.40% Salinity.
(Natural Concentration)
One series. Filtered through coarse filter paper.

1 $C_p = 0.9526 + 1.3457 \times 10^{-4} T$ $\sigma = 5.5 \times 10^{-4}$

2 $C_p = 0.9533 + 8.058 \times 10^{-5} T + 6.423 \times 10^{-7} T^2$ $\sigma = 4.7 \times 10^{-4}$

$\triangle$ CALC. FROM COX AND SMITH EQUATION

C_p, cal/g-°C

T, °C

Figure 14 Heat Capacities of La Jolla Sea Water Concentrate at 5.01 % Salinity. (Approximately $1\frac{1}{2}$ times normal) One series. Filtered through coarse filter paper.

1 $C_p = 0.9336 + 1.5569 \times 10^{-4} T$ $\sigma = 6.4 \times 10^{-4}$

2 $C_p = 0.9323 + 2.5301 \times 10^{-4} T - 1.1439 \times 10^{-6} T^2$ $\sigma = 3.0 \times 10^{-4}$

(23)
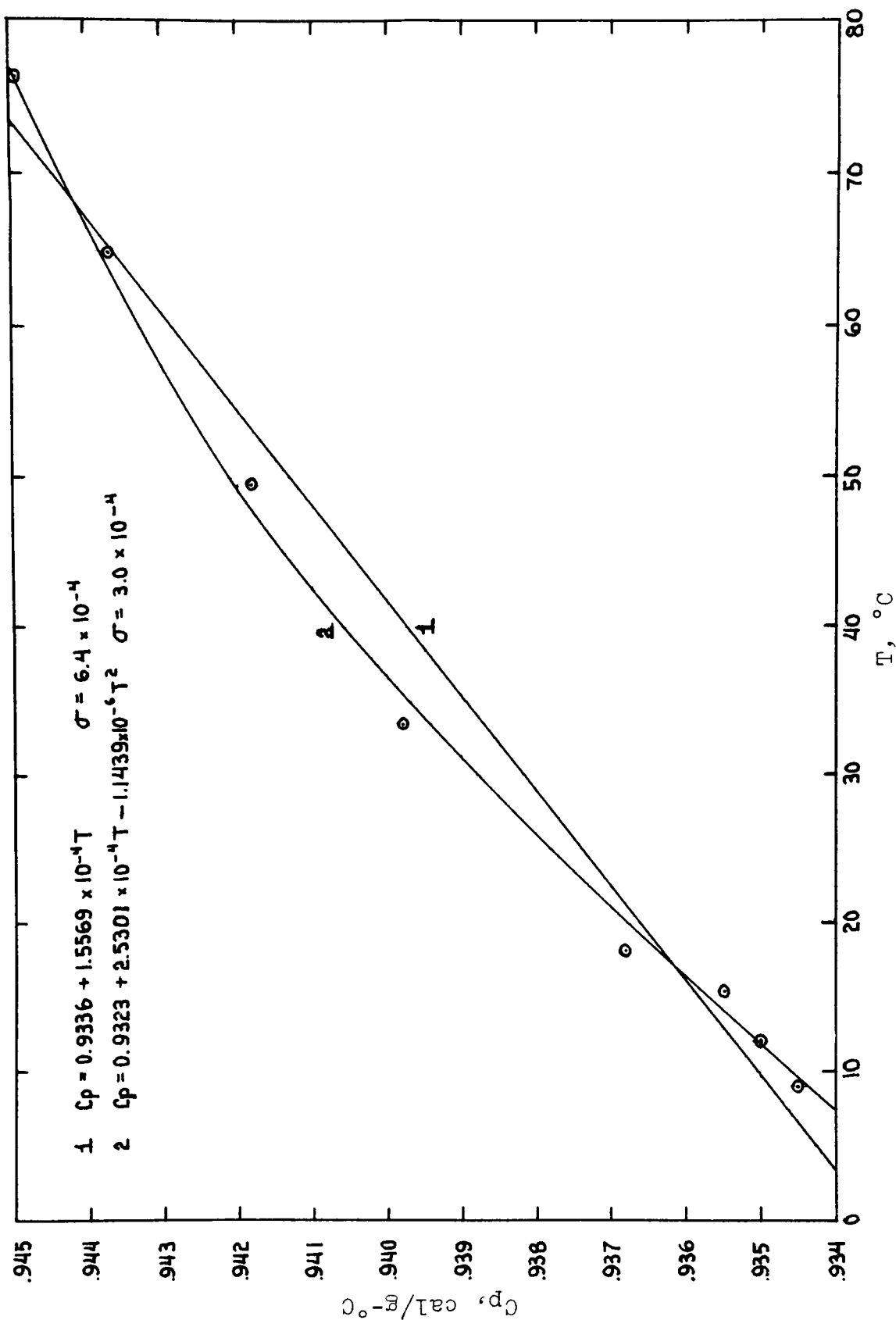
Figure 15 Heat Capacities of La Jolla Sea Water Concentrate at 6.67% Salinity. (Approximately double normal) Three series. All three samples treated in laboratory by filtering through coarse filter paper and acidifying to 4.5 pH.

1 $C_p = 0.9149 + 1.7771 \times 10^{-4} T$ $\sigma = 9.6 \times 10^{-4}$

2 $C_p = 0.9126 + 3.3066 \times 10^{-4} T - 1.7720 \times 10^{-6} T^2$ $\sigma = 5.6 \times 10^{-4}$

(24)

Figure 16 Heat Capacities of La Jolla Sea Water Concentrate at 8.3% Salinity. (Approximately 2½ times normal) One series. Treated in laboratory by filtering through coarse filter paper and acidifying to 4.5 pH.

1 $C_p = 0.8967 + 2.080T \times 10^{-4}T$ $\sigma = 1.04 \times 10^{-3}$

2 $C_p = 0.8947 + 3.6026 \times 10^{-4}T - 1.8070 \times 10^{-6}T^2$ $\sigma = 4.0 \times 10^{-4}$

(25)

Figure 17 Heat Capacities of La Jolla Sea Water Concentrate at 9.96% Salinity. (Approximately three times normal) Two series. One sample filtered through diatomaceous earth, acid-ified to 4.5 pH, and deaerated to 5.9 pH; the other sample treated in the laboratory by filtering through coarse filter paper and acidifying to 4.5 pH.

1 $C_p = 0.8813 + 1.8619 \times 10^{-4}\,T$ $\sigma = 7.2 \times 10^{-4}$

2 $C_p = 0.8796 + 3.0222 \times 10^{-4}\,T - 1.3162 \times 10^{-6}\,T^2$ $\sigma = 4.4 \times 10^{-4}$

(26)

Figure 18 Heat Capacities of La Jolla Sea Water Concentrate at 10.10% Salinity. (Approximately three times normal) Three series. Each sample filtered through diatomaceous earth, acidified to 4.5 pH and deaerated to 6.0 - 6.2 pH.

1 $C_p = 0.8803 + 1.7835 \times 10^{-4} T$ $\sigma = 1.39 \times 10^{-3}$

2 $C_p = 0.8779 + 3.5097 \times 10^{-4} T - 2.0618 \times 10^{-6} T^2$ $\sigma = 9.5 \times 10^{-4}$

Figure 19 Heat Capacities of La Jolla Sea Water Concentrate at 11.40% Salinity. (Approximately 3½ times normal) One series. Sample filtered through diatomaceous earth, acidified to 4.5 pH, deaerated to 6.0 pH.

1 $C_P = 0.8670 + 2.0320 \times 10^{-4} T$ $\sigma = 1.42 \times 10^{-3}$

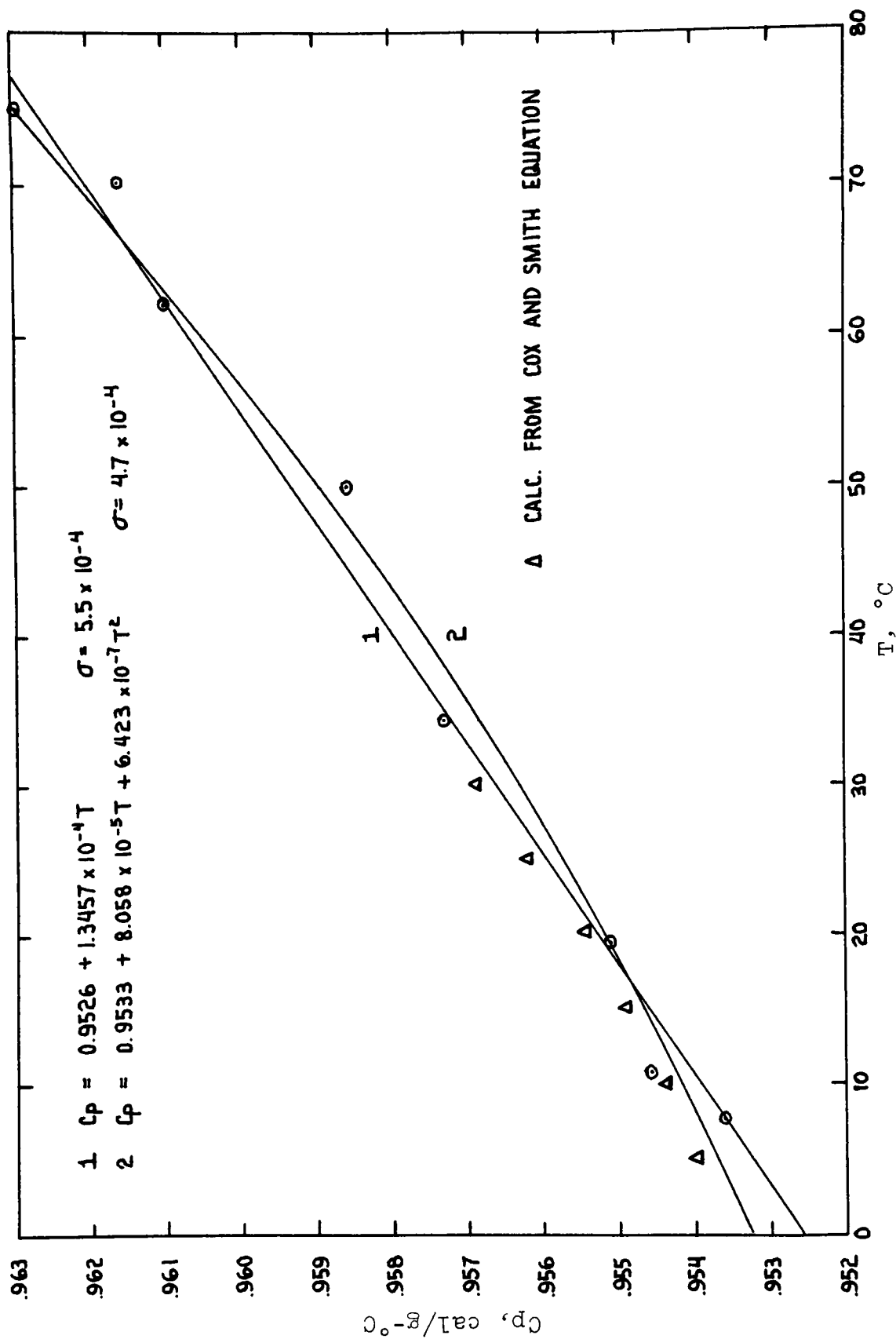2 $C_P = 0.8648 + 3.9930 \times 10^{-4} T - 2.5106 \times 10^{-6} T^2$ $\sigma = 5.5 \times 10^{-4}$
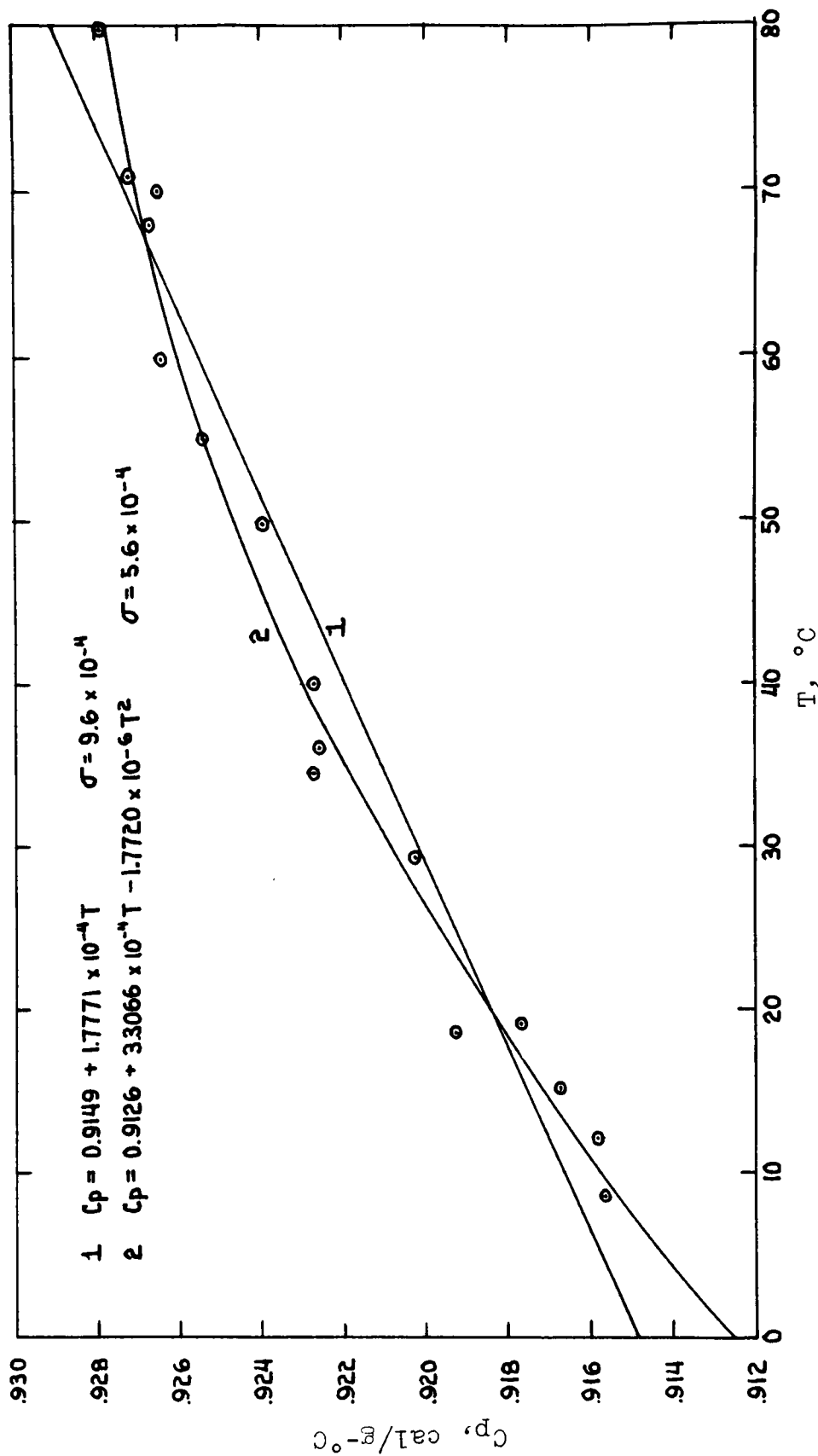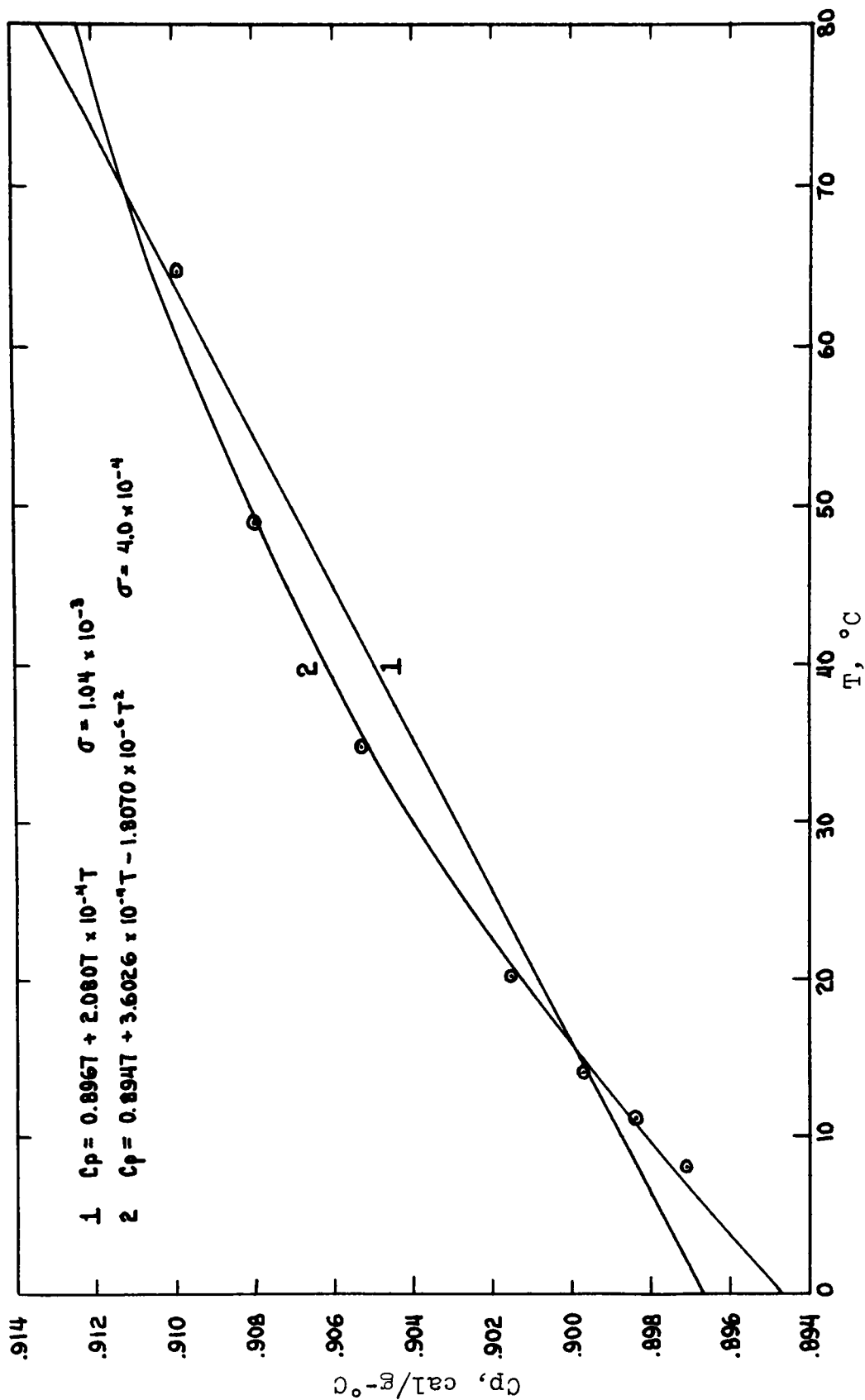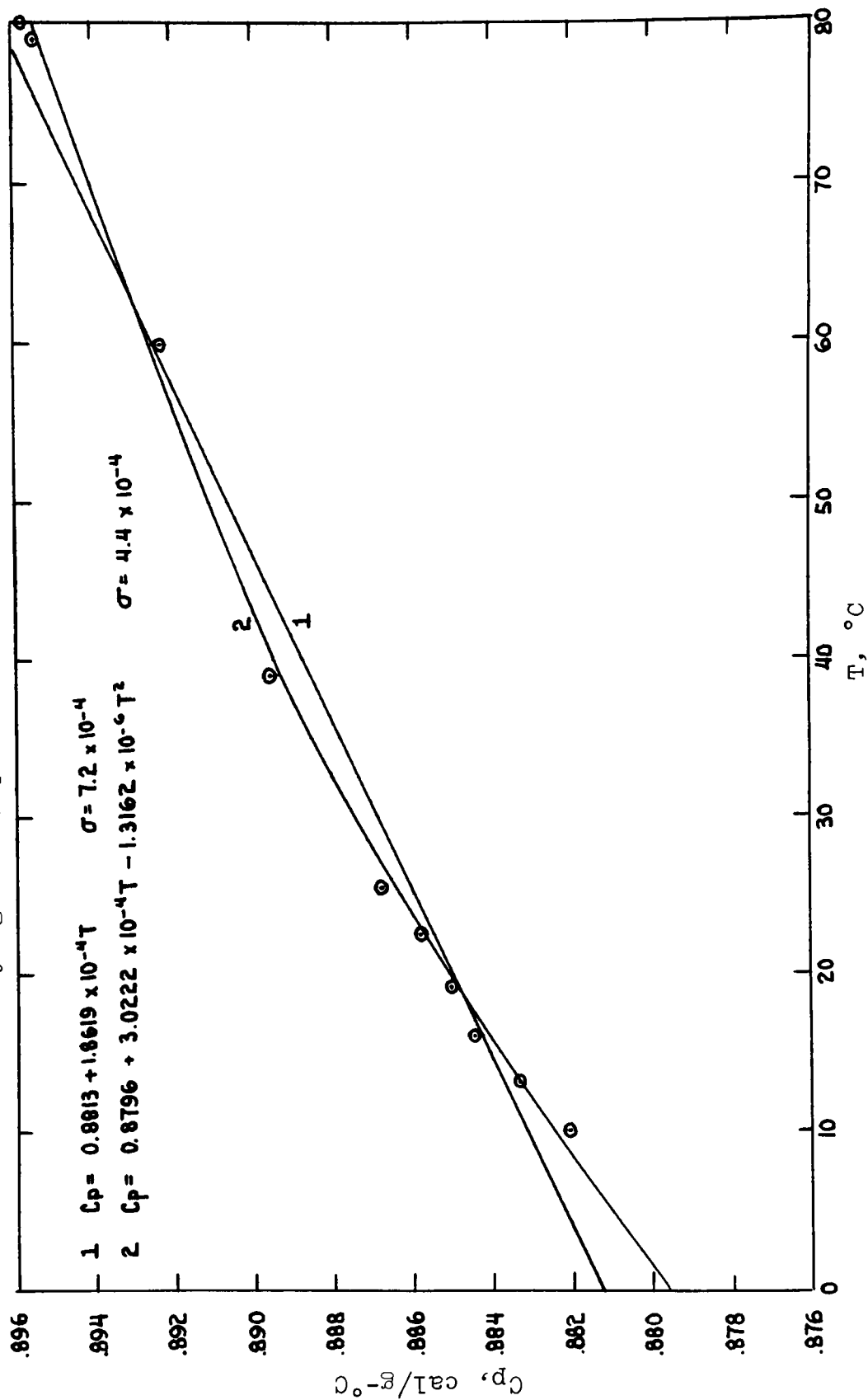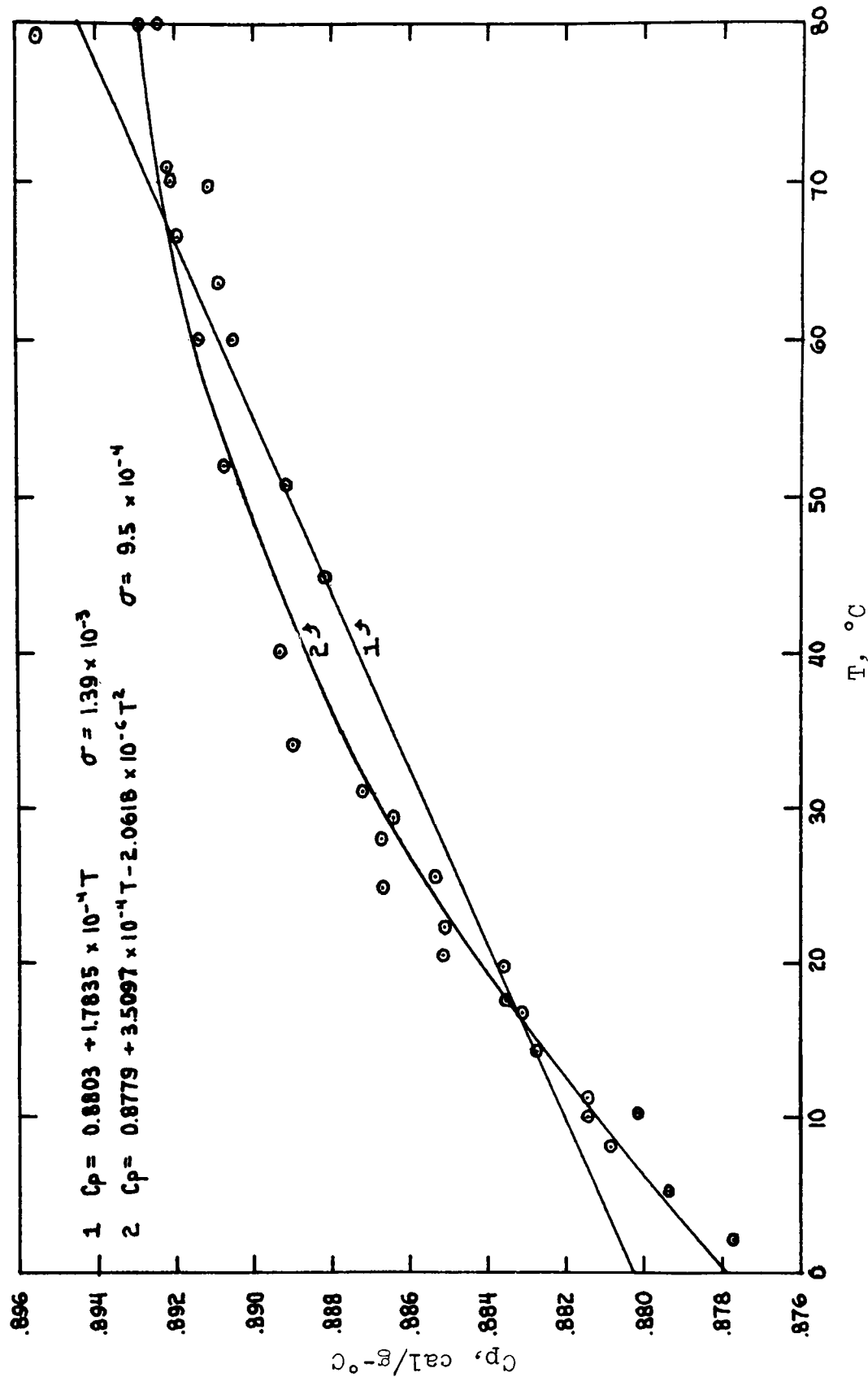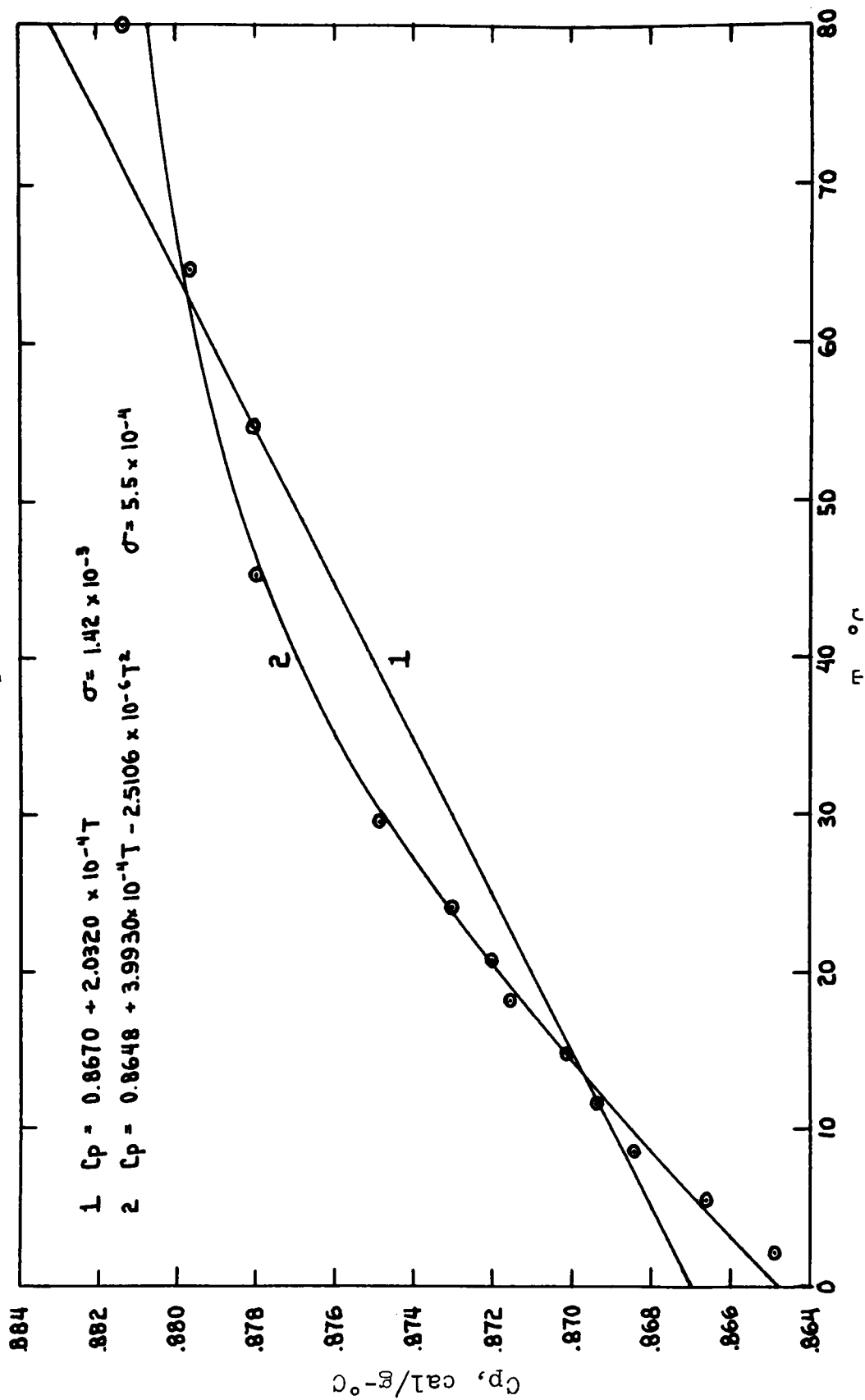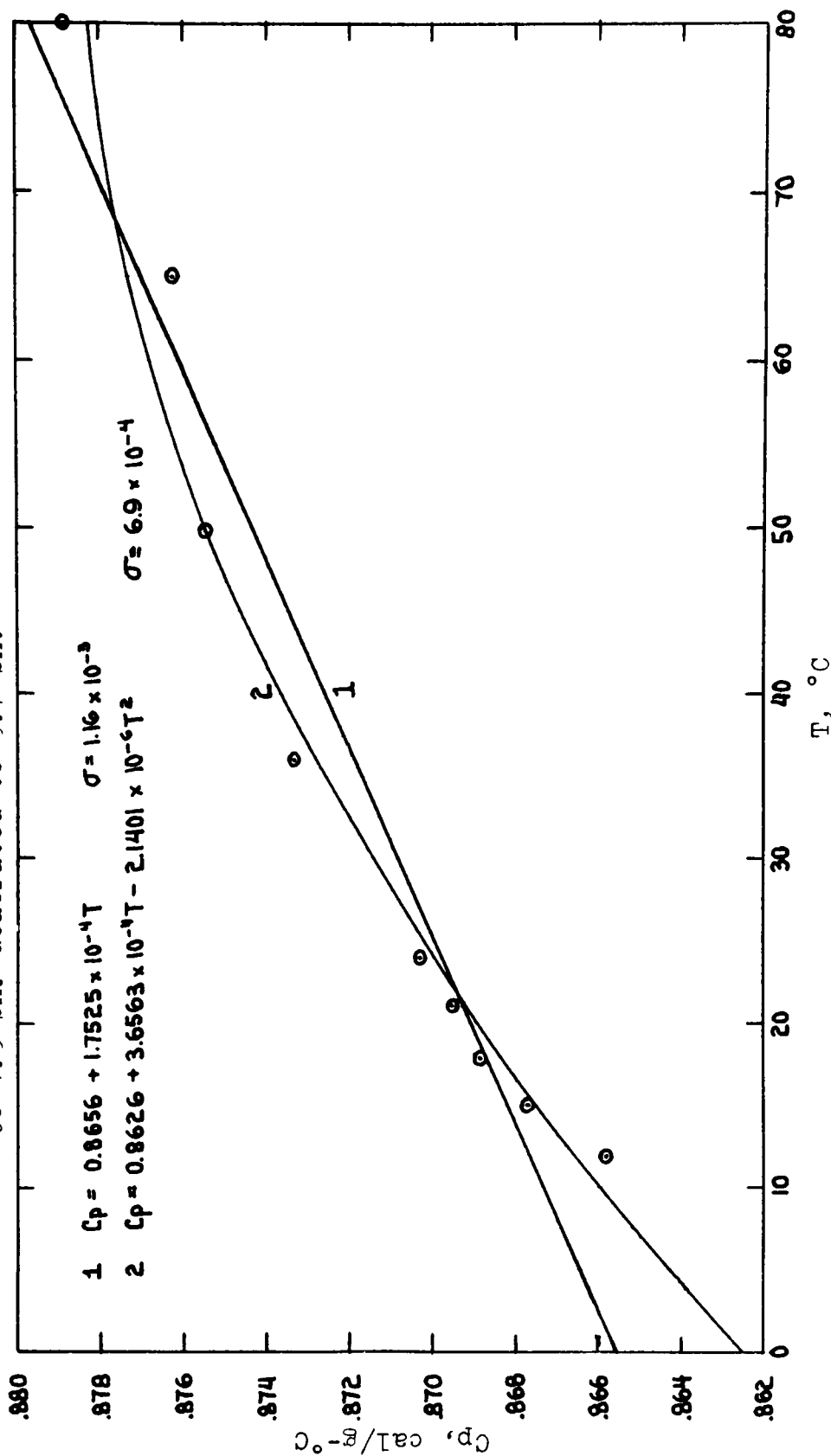
Figure 20 Heat Capacities of La Jolla Sea Water Concentrate at 11.74% Salinity. (Approximately 3½ times normal) One series. Sample filtered through diatomaceous earth, acidified to 4.5 pH; deaerated to 5.7 pH.

1 $C_p = 0.8656 + 1.7525 \times 10^{-4} T$ $\sigma = 1.16 \times 10^{-3}$

2 $C_p = 0.8626 + 3.6563 \times 10^{-4} T - 2.1401 \times 10^{-6} T^2$ $\sigma = 6.9 \times 10^{-4}$

The final column of the table presents the ratio of the two standard deviations. The closer the value of the ratio is to 1, the more nearly accurately the data are described by the linear equation. Below natural sea water concentration (~3.36%), a quadratic curve is required to provide a fit approaching an accuracy of one part per thousand, our estimated experimental error. Above normal sea water concentration, a straight line gives a reasonably good fit to the data, but the quadratic curve yields a substantially lower standard deviation.

Figures 10, 11, and 13 contain points calculated from the equation of Cox and Smith[1]:

$$C_p = A - (1.2130 \times 10^{-2}S) - (3.346 \times 10^{-4}S^2)$$

where C_p is the heat capacity in calories/gram-°C for sea water of salinity S at temperature T°C, and A is the heat capacity of pure water at temperature (T + 7.0S + 1.75S²)°C. The original Cox and Smith equation is given with heat capacity in absolute joules/gram-°C, and salinity in grams/kilogram sea water. The equation as shown above has been converted to give heat capacities in calories/gram-°C, with salinity in percent, to conform with the units used in treating our own data. Their equation is based on experimental data up to 30°C, over a salinity range of 0-4%. Agreement between their work and ours is excellent. Figure 11 presents 24 of Cox' and Smith's actual experimental points at 3.005% salinity. The curve defined by their equation, as well as all but two of their experimental values, falls within one part per thousand of our least squares curves.

Extrapolation of the Cox and Smith equation beyond their temperature and concentration range should not be attempted. Calculated values are too high at higher temperatures. This is shown in Figure 11 by the dashed line which represents the curve calculated from their equation.

Figure 12 presents points for a number of different samples of natural sea water, for which the salinity varied from 3.34% to 3.38%. Variables investigated during these various runs included the following: two different experimenters; modifications in the apparatus which altered the effective heat capacity of the system as determined by calibration; different pretreatment of the sample, contrasting a simple filtration through coarse filter paper with a more complex treatment consisting of filtering through diatomaceous earth followed by acidification with sulfuric acid and deaeration. The

agreement among these various runs is convincing evidence that none of these variables introduced differences which affected the results beyond the experimental error of one part per thousand. Of particular importance is the observation that acidification does not alter the results. As has been mentioned, all 3- and 3½-times concentrated sea waters were acidified with concentrated sulfuric acid to prevent the precipitation of salts during concentration. The amount of acid added increased the sulfate ion concentration from about 7.7% of total solids in natural sea water to 8.0% of the total solids in the acidified sea water. This was not sufficient to affect the heat capacity of the sea water. It may thus be concluded that the heat capacity of the concentrate is similarly not affected.

Figure 13 shows the data for the sea water sample obtained at the equator. Heat capacities for this sample agreed well within experimental error with those calculated for a salinity of 3.40%, based on the results with La Jolla sea water. From these limited data, it may be concluded that the salinity of the water is the controlling factor in determining the heat capacity, rather than its source or possible difference in organic content. Samples have been requested from the North Pacific and from the Atlantic; these will provide additional evidence of the effect of sample source.

Figures 14-20 illustrate that, for sea water concentrates, the nonlinearity of the temperature coefficient of heat capacities is not as marked as it is for sea water dilutions. The degree of curvature that does exist is in the opposite direction (concave to the temperature axis) from that of sea water dilutions. This trend was observed consistently for all concentrates.

Sodium Chloride Solutions (Figures 21-23)

These figures present our experimental points for sodium chloride solutions. Concentrations approximating normal, twice normal, and three times the concentration of La Jolla sea water were selected. The triangular points at 25°, and in two cases also at 45°, represent calculated values from least squares equations we obtained using data in the literature; namely, those of Randall and Rossini[8] and those of Hess and Gramkee[9]. Randall and Rossini data extend across and well beyond our concentration range, but are limited to 25°C. Hess and Gramkee data include temperatures from 15 to 45°, but their concentration range is not high enough to include our 1.836M NaCl solution. The equations are as follows:

Figure 21 Heat Capacities of Sodium Chloride Solution at 3.48% Salinity (0.617 Molar). (Approximates natural sea water).

1 $C_p = 0.9543 + 1.1038 \times 10^{-4} T$ $\sigma = 4.8 \times 10^{-4}$

2 $C_p = 0.9533 + 1.7225 \times 10^{-4} T - 7.601 \times 10^{-7} T^2$ $\sigma = 4.4 \times 10^{-4}$

▽ at 25°, 45°   Hess and Gramkee

△ at 25°   Randall and Rossini

C_p, cal/g-°C

T, °C

(32)

Figure 22 Heat Capacities of Sodium Chloride Solution at 6.73% Salinity
(1.234 Molar).
(Approximates doubly concentrated sea water).

1 $C_p = 0.9184 + 1.3870 \times 10^{-4} T$ $\sigma = 9.4 \times 10^{-4}$

2 $C_p = 0.9150 + 3.5771 \times 10^{-4} T - 2.7208 \times 10^{-6} T^2$ $\sigma = 3.9 \times 10^{-4}$

$\triangledown$ at 25°, 45°   Hess and Gramkee

$\triangle$ at 25°   Randall and Rossini
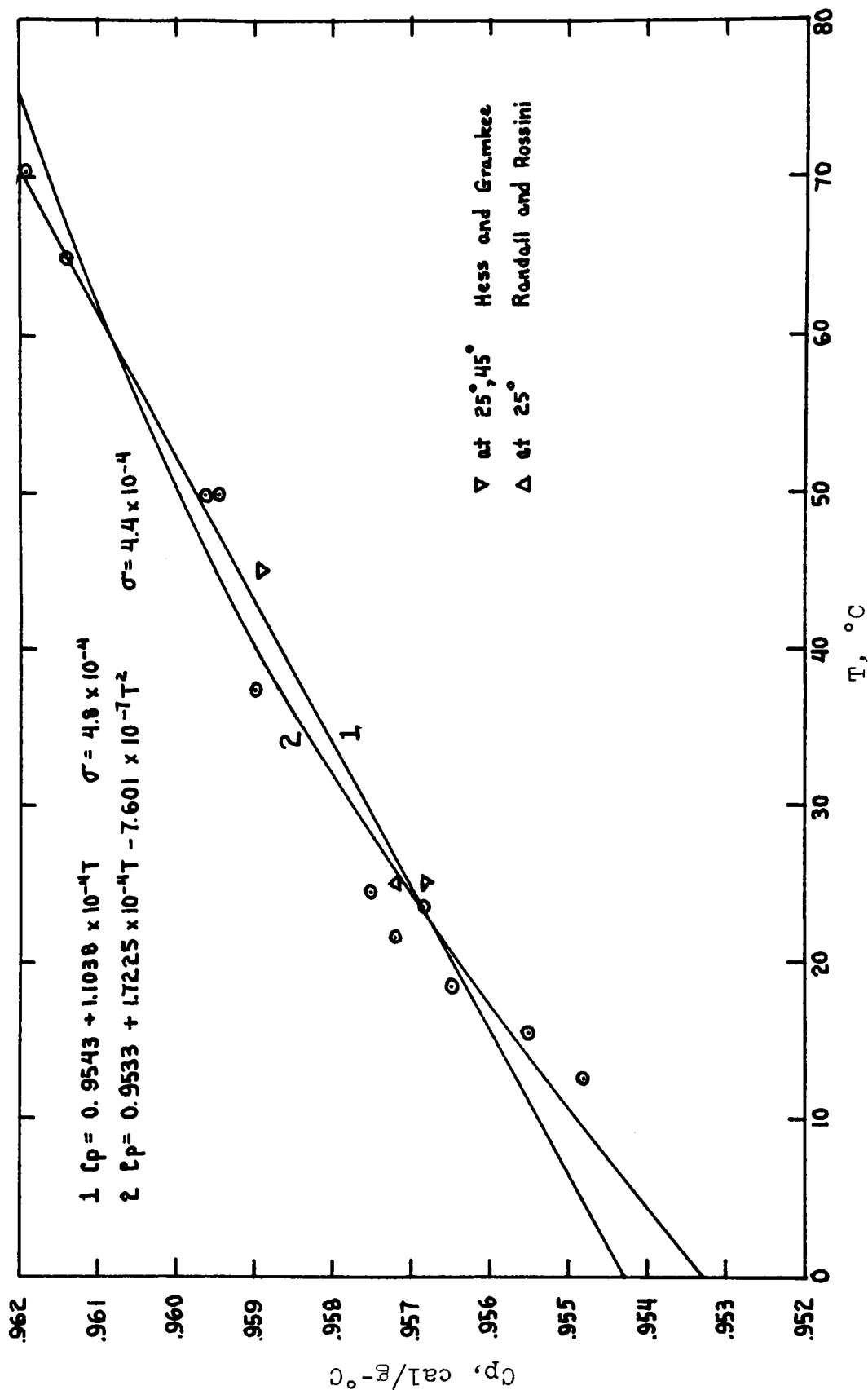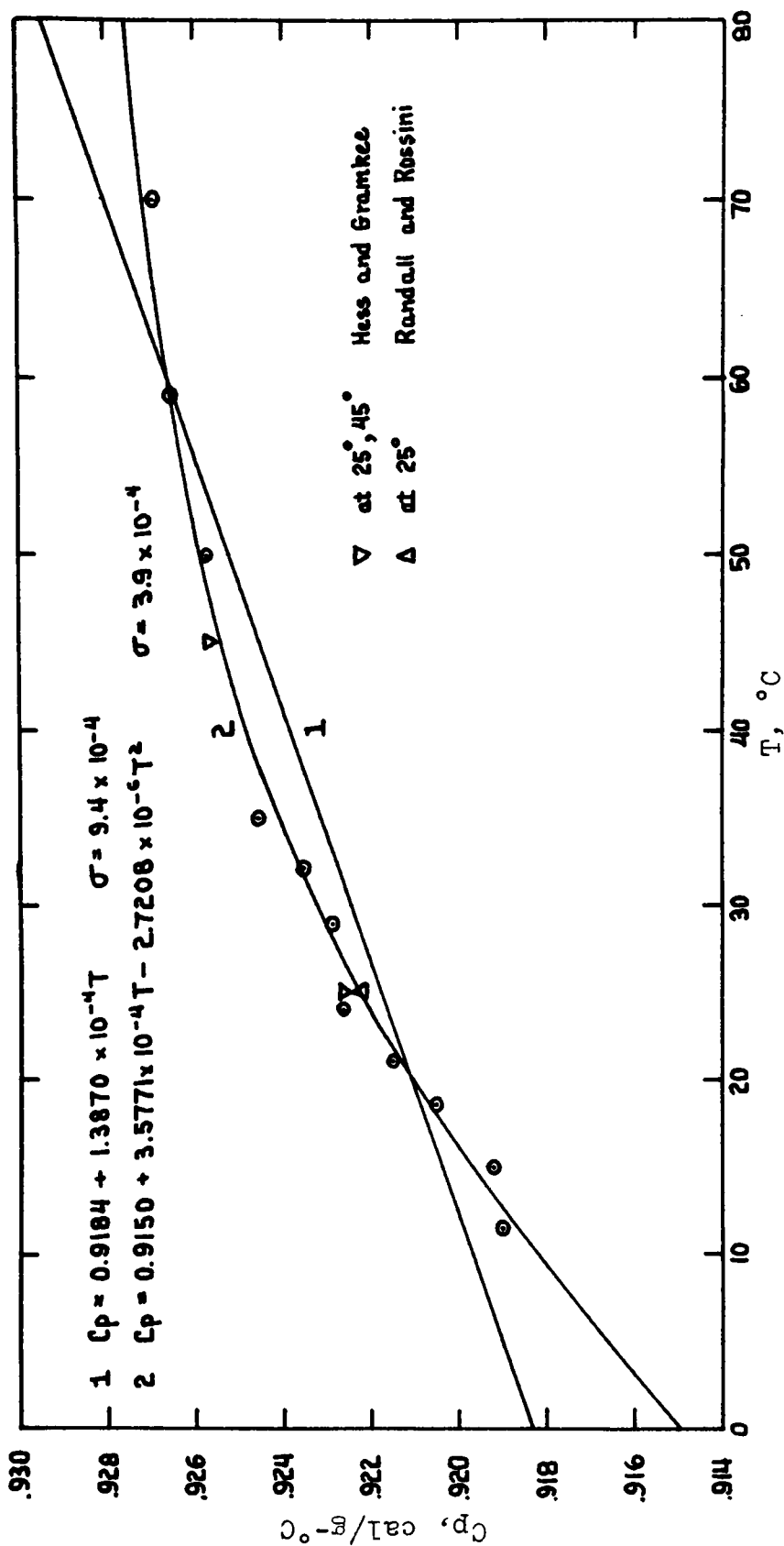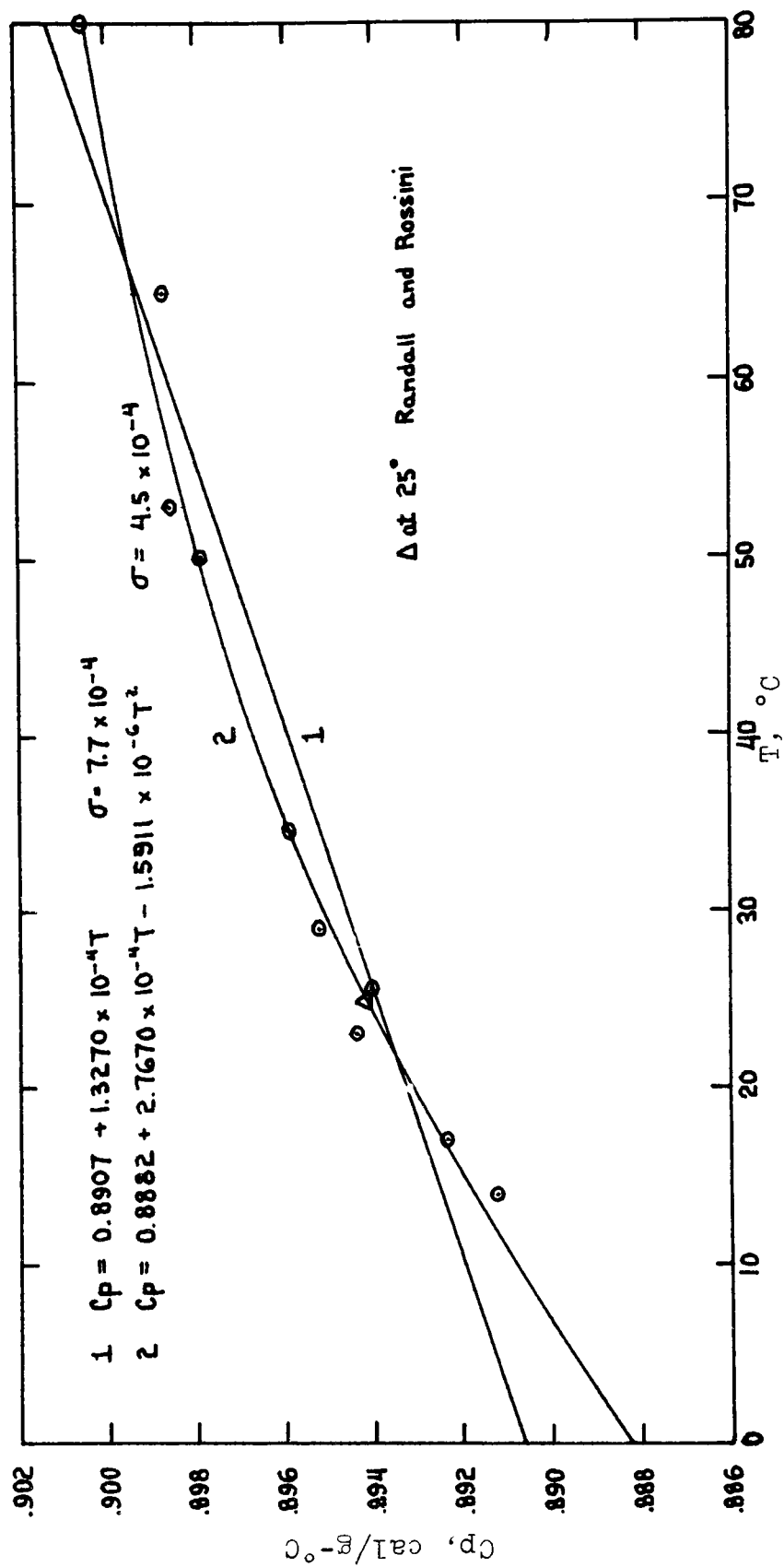
Figure 23 Heat Capacities of Sodium Chloride Solution at 9.69% Salinity (1.836 Molar). (Approximates triply concentrated sea water).

1 $C_P = 0.8907 + 1.3270 \times 10^{-4} T$ $\sigma = 7.7 \times 10^{-4}$
2 $C_P = 0.8882 + 2.7670 \times 10^{-4} T - 1.5911 \times 10^{-6} T^2$ $\sigma = 4.5 \times 10^{-4}$

$\triangle$ at 25° Randall and Rossini

C_P, cal/g-°C

T, °C

(34)

From Randall and Rossini data:

$$c_p^{25} = 0.9974 - 0.071605X + 0.0081036X^2$$

From Hess and Gramkee data:

$$c_p^{25} = 0.9979 - 0.07490X + 0.01074X^2$$

$$c_p^{45} = 0.9986 - 0.07274X + 0.010404X^2$$

where X is molality and C_p is heat capacity for NaCl solutions.

These two pairs of investigators used earlier values for distilled water as their reference point, which are lower by about one part per thousand than those of Osborne, Stimson, and Ginnings used in the present work. Thus, their heat capacity values have had to be adjusted upwards by a corresponding amount, in order to be compared with ours. The points shown on the figures have been so adjusted. Agreement between the present values and those of the previous investigators is excellent. In all cases their points lie well within one part per thousand of ours.

At concentrations higher than that of natural sea water, deviations are apparent between the temperature dependence of the heat capacities of sea water and that of the corresponding NaCl solutions. This is in accord with the observation that other ions exhibit a stronger dependence than do the Na^+ or Cl^- ions. This will be discussed further in the following section.

Synthetic Sea Water

A synthetic sea water containing Na^+, Mg^{++}, Cl^-, and $SO_4^=$ ions as described on page 11 was prepared to simulate triply concentrated natural sea water. The number of ions were identical for the two solutions; the % salinity for the synthetic solution was 9.53% in contrast with 10.1% for the natural sea water. The experimental data are shown in Figure 24. It may be seen by comparing this figure with Figures 18 and 23 that the synthetic sea water approaches the behavior* of natural sea water at this concentration considerably more closely than does the NaCl solution. This confirms that at increasing concentrations, the presence of other ions exerts a significant effect on the heat capacities. Additional evidence is shown in Figure 25, where data are presented for a 1.40% Na_2SO_4

*i.e., the temperature variation of heat capacity

Figure 24 Heat Capacities of a Synthetic Sea Water at 9.53% Salinity. (Monovalent ions of sea water replaced by Na^+ and Cl^-; divalent, by Mg^{++} and $SO_4^=$, to approximate triply concentrated sea water)

1 $C_p = 0.8865 + 2.1150 \times 10^{-4} T$ $\sigma = 1.1 \times 10^{-3}$

2 $C_p = 0.8851 + 3.4743 \times 10^{-4} T - 1.7109 \times 10^{-6} T^2$ $\sigma = 5.5 \times 10^{-4}$
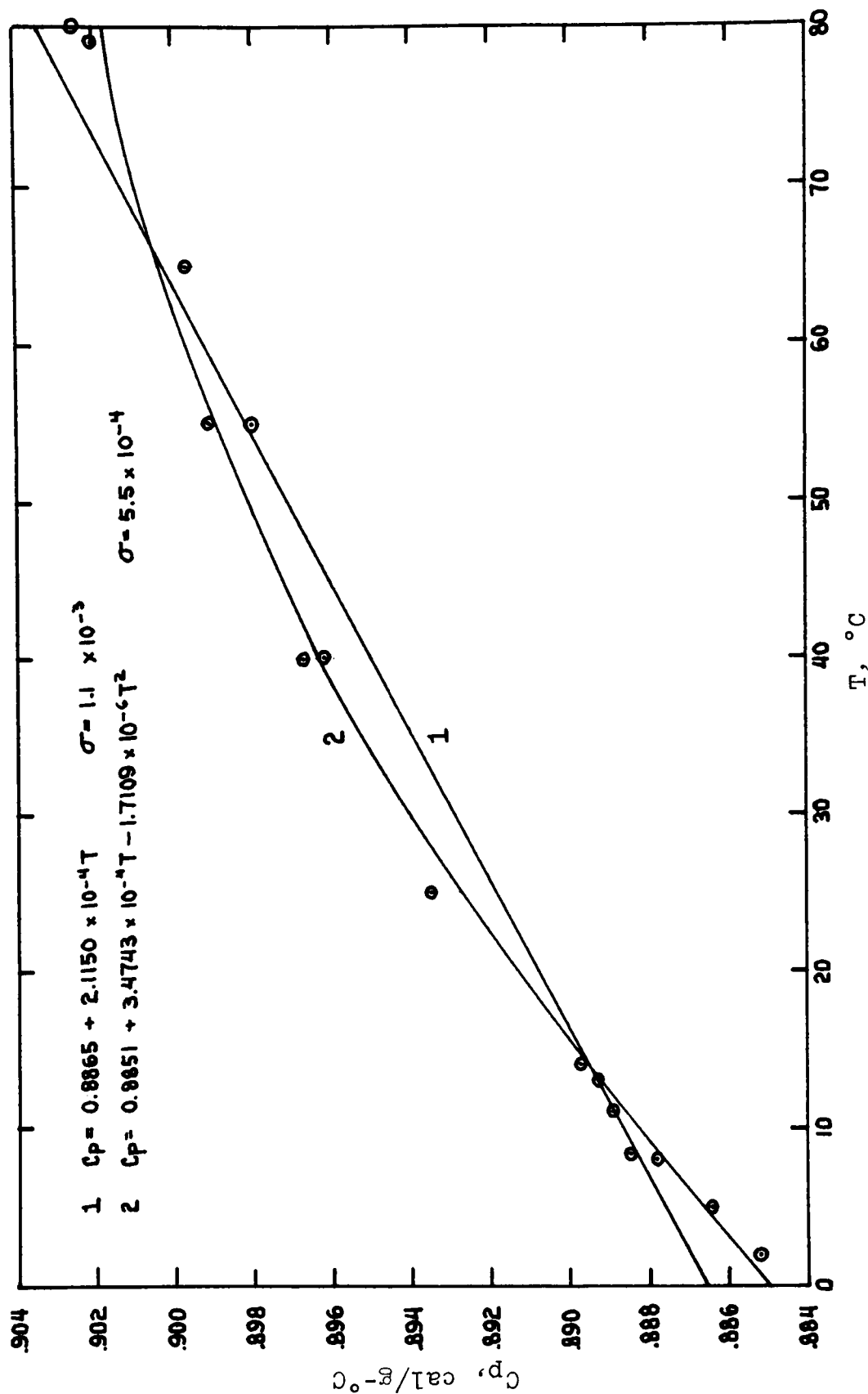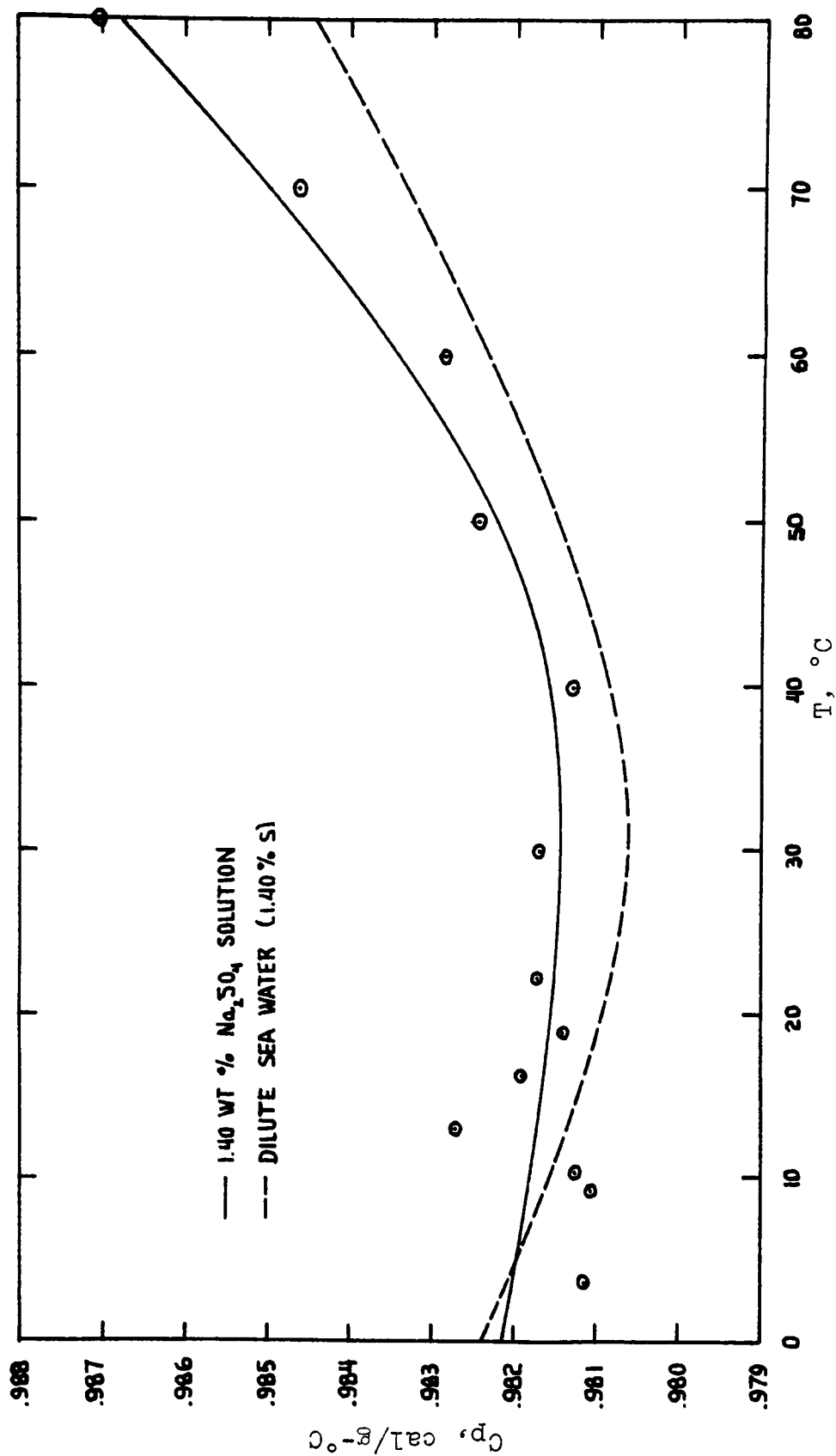
(36)

Figure 25 Temperature Dependence of Heat Capacities of a Dilute Solution
of Na_2SO_4 Compared with that of a Dilute Sea Water.

(37)

solution. Comparison with sea water at the same weight percent salinity indicates that the heat capacities of the Na_2SO_4 solution have a stronger temperature dependence. This will be discussed further in the section on Discussion and Conclusions.

DISCUSSION (TEMPERATURE RANGE OF 2-80°C)

Sea Water Solutions

Heat Capacities of Sea Water as a Combined Function of Temperature and Concentration

In Figure 26 are assembled the curves previously presented of heat capacity as a function of temperature at various salinities. These curves will not be discussed here inasmuch as they have received detailed attention in the section on Experimental Results. Figure 27 presents the data in the form of three isotherms: 0° (extrapolated), 25°, and 80°, showing heat capacity as a function of concentration. The extrapolation of the data to 0° appeared justified because experimental points were obtained as low as 2-5°C. The following may be observed from the figure:

(1) Heat capacity is lowered by about 0.0125 calories/gram-°C for each 1% increase in salinity.

(2) The overall change in heat capacity across the temperature range of 0-80° is greatest at 6% salinity and above. In this concentration range, the average increase in heat capacity is about 0.001 calories per five degree rise in temperature.

(3) The relationship of heat capacity with temperature, as also with salinity, is nonlinear.

Equations and Nomograph

Figures 6-20 have presented the linear and quadratic equations of heat capacity as a function of temperature, obtained by least squares fitting of the data. The constants for these equations are tabulated in Table 5. These values were in turn used to derive equations for heat capacity as a combined function of temperature and salinity. Equations of varying degrees of complexity are listed in Table 6.

In addition, a nomograph has been constructed and is shown as Figure 28. The nomograph and the equations are valid

(38)

Figure 26 Heat Capacity of Sea Water Solutions.

(39)

(66)
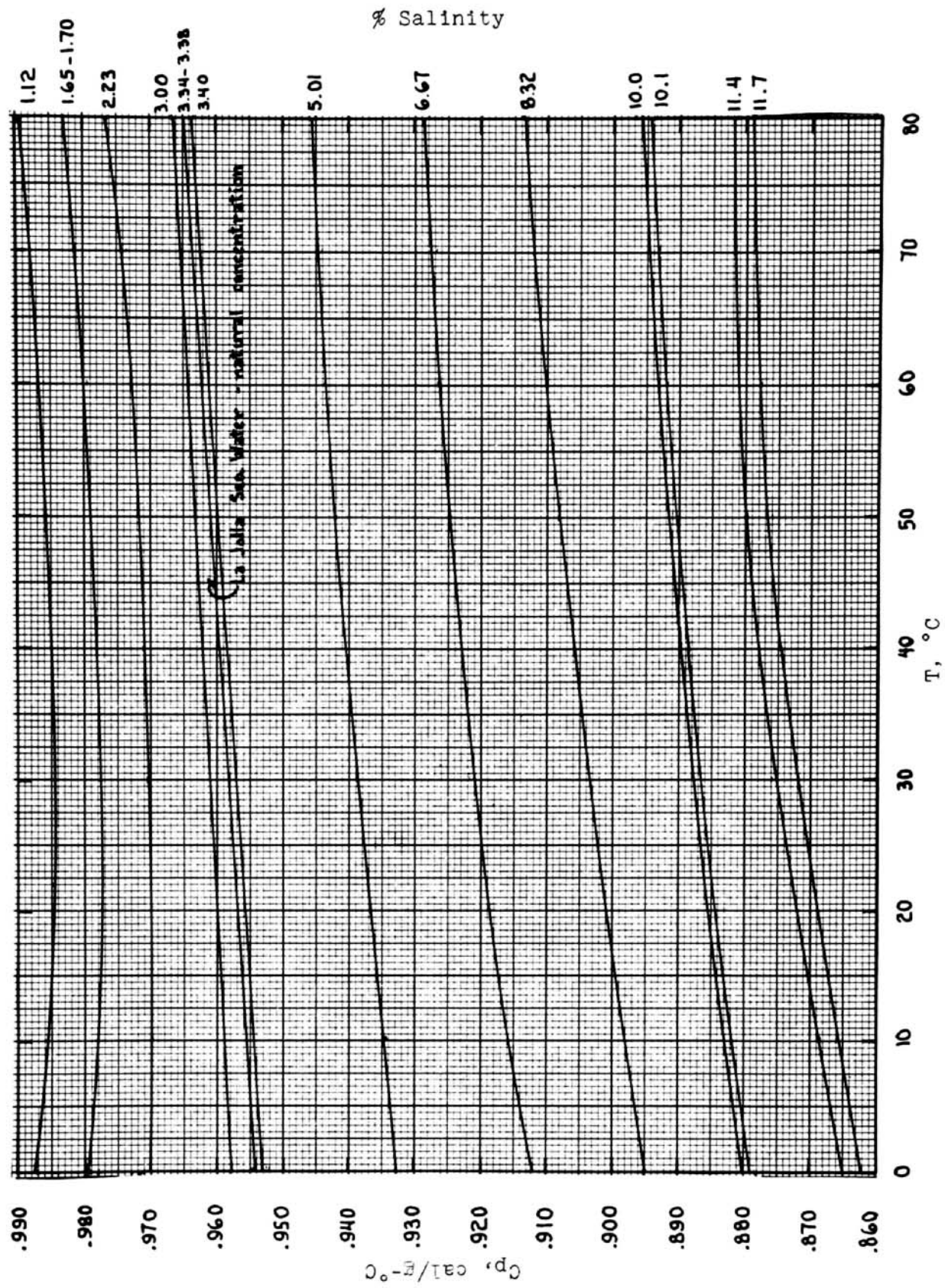
Figure 27   Heat Capacity of Sea Water as a
Function of Concentration
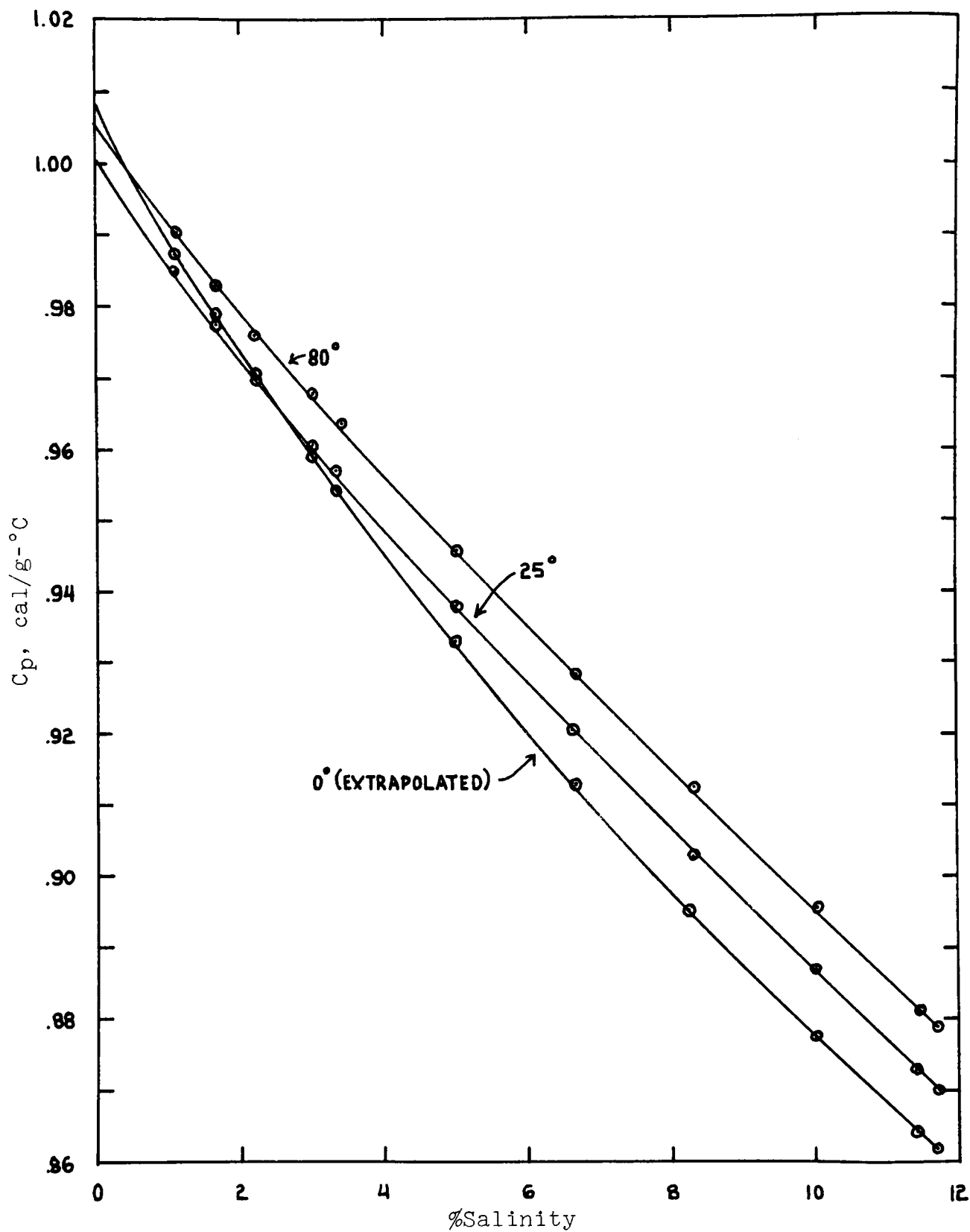
Table 5

CONSTANTS FOR LINEAR AND QUADRATIC EQUATIONS FOR C_p AS A FUNCTION OF T

Salinity, %	Linear: $C_p = A + BT$		Quadratic: $C_p = C + DT + ET^2$		
	A	$B \times 10^4$	C	$D \times 10^4$	$E \times 10^6$
0	1.0019	-0.26373	1.0060	-3.5810	4.1465
1.12	0.9844	0.44645	0.9872	-1.5295	2.3553
1.65	0.9763	0.6758	0.9793	-1.2071	2.0986
1.69	0.9764	0.5485	0.9782	-0.8625	1.8148
1.70	0.9759	0.5052	0.9776	-0.8907	1.8249
2.23	0.9687	0.8604	0.9700	-0.05175	1.0614
3.00	0.9579	1.1410	0.9583	0.5950	0.8158
3.36	0.9546	1.1349	0.9553	0.6381	0.5605
3.40*	0.9526	1.3457	0.9533	0.8058	0.6423
5.01	0.9336	1.5569	0.9323	2.5301	-1.1439
6.67	0.9149	1.7771	0.9126	3.3066	-1.7720
8.32	0.8967	2.0807	0.8947	3.6026	-1.8070
9.96	0.8813	1.8619	0.8796	3.0222	-1.3162
10.10	0.8803	1.7835	0.8779	3.5097	-2.0618
11.40	0.8670	2.0320	0.8648	3.993	-2.5106
11.74	0.8656	1.7525	0.8626	3.6563	-2.1401

* equatorial sample

Table 6

EQUATIONS OF HEAT CAPACITY AS A COMBINED FUNCTION OF TEMPERATURE AND SALINITY

1. $C_p = 0.9948 - 0.011412S + [(0.42997 + 0.15192S) \times 10^{-4}T]$ *

2. $C_p = 1.0007 - 0.014880S + (2.8618 \times 10^{-4}S^2) + [(0.42997 + 0.15192S) \times 10^{-4}T]$

3. $C_p = 0.9975 - 0.011932S - [(1.6371 - 0.5376S) \times 10^{-4}T] + [(2.5295 - 0.46594S) \times 10^{-6}T^2]$

4. $C_p = 1.0007 - 0.014880S + (2.8618 \times 10^{-4}S^2) - [(0.14054 - 0.48497S + 0.027454S^2) \times 10^{-4}T]$

5. $C_p = 1.0049 - 0.016210S + (3.5261 \times 10^{-4}S^2) - [(3.2506 - 1.47955S + 0.07765S^2) \times 10^{-4}T] + [(3.8013 - 1.2084S + 0.06121S^2) \times 10^{-6}T^2]$

* $C_p = cal/g-°C;$ $S = percent\ salinity;$ $T = °C$

(42)

PERCENT
SALINITY

Cp,
CAL/GRAM-°C

TEMPERATURE,
°C

Accuracy within:

0 to ±0.003 cal for 1-12%S at 0-80°C
and for 0-1%S at 10-80°C

±0.003-0.010 cal for <1%S at <10°C

Figure 28
Nomograph for Estimating Heat Capacities of Sea Water
at 0-12% Salinity and 0-80°C

(43)
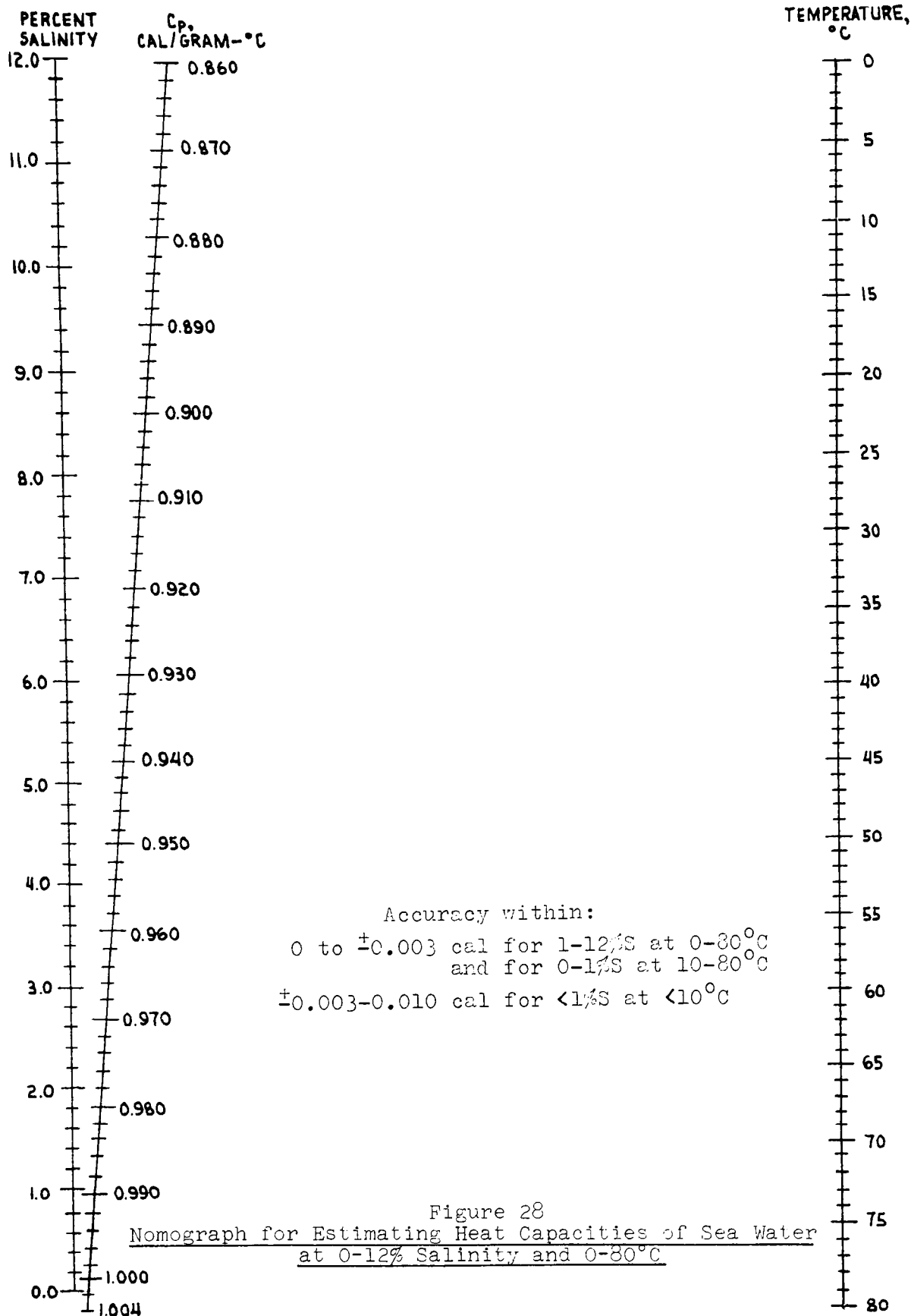
over a temperature range of 0-80°C and a salinity range
of 0-12%. Table 7 is presented to illustrate the accuracy
of the nomograph and equations in yielding the experimen-
tal values for heat capacity. Heat capacities from the
least squares quadratic curves of the experimental data for
seven   concentrations and five temperatures are compared
with values estimated from the nomograph and those calcula-
ted from each of the five general equations of Table 6.
The column labelled "ΔC_p" lists the differences between
the experimental and estimated or calculated values. By
scanning Table 7, one can observe that the nomograph
generally gives an accuracy of two parts per thousand or
better. The complex Equation 5 is accurate to within about
one part per thousand, and the simpler Equation 4 is almost
as accurate--one part per thousand or better eighty per-
cent of the time. The accuracies are tabulated in Table
8, as the number of times out of the thirty-five selected
points the indicated accuracy was reached.

<div align="center">Table 8</div>

<div align="center">ACCURACY OF NOMOGRAPH AND EQUATIONS IN YIELDING CORRECT
VALUES OF HEAT CAPACITIES</div>

Equation or Nomograph	Number times Indicated Accuracy was Obtained				
	$\Delta C_p* = $ 0.000	0.001	0.002	0.003	0.004 or more
Nomograph	11	14	5	3	2
Eq. 1 (4 terms)	7	8	7	6	7
Eq. 2 (5 terms)	4	16	7	6	2
Eq. 3 (6 terms)	5	12	5	5	8
Eq. 4 (6 terms)	13	15	3	3	1
Eq. 5 (9 terms)	22	11	1	1	0

* C_p in calories/gram-°C

Equations in which $C_{p_{T=0}}$ is expressed as a linear function
of salinity, of which Equations 1 and 3 are examples, are
considerably less satisfactory than those in which it is
expressed as a quadratic function of salinity. This, of
course, is a reflection of the pronounced difference in
curvature in the low temperature regions at various sali-
nity: C_p decreases as temperature increases from 0-20° at
salinities below 2%, and rises in the same temperature

Table 7
COMPARISON BETWEEN EXPERIMENTAL HEAT CAPACITIES WITH THOSE ESTIMATED FROM NOMOGRAPH OR CALCULATED FROM EQUATIONS

Cp, cal/g-°C

S,%	T,°C	Exptal	Nomograph*	ΔCp	Eq.1**	ΔCp	Eq.2	ΔCp	Eq.3	ΔCp	Eq.4	ΔCp	Eq.5	ΔCp
0	0	1.008	.998	.010	.995	.013	1.001	.007	.998	.010	1.001	.007	1.005	.003
0	10	1.002	.999	.003	.995	.007	1.001	.001	.996	.006	1.001	.001	1.002	.000
0	25	.999	.999	.000	.996	.003	1.002	.003	.995	.004	1.000	.001	.999	.000
0	50	.999	1.000	.001	.997	.002	1.003	.004	.996	.003	1.000	.001	.998	.001
0	80	1.003	1.002	.001	.998	.005	1.004	.001	1.001	.002	1.000	.000	1.003	.000
1.12	0	.987	.984	.003	.982	.005	.984	.003	.984	.003	.984	.003	.987	.000
1.12	10	.986	.985	.001	.983	.003	.985	.001	.983	.003	.985	.001	.986	.000
1.12	25	.985	.986	.001	.984	.001	.986	.001	.983	.002	.985	.000	.985	.000
1.12	50	.985	.987	.002	.985	.000	.987	.002	.984	.001	.986	.001	.995	.000
1.12	80	.990	.989	.001	.987	.003	.989	.001	.989	.001	.987	.003	.990	.001
2.23	0	.970	.970	.000	.970	.000	.968	.002	.971	.001	.969	.001	.971	.000
2.23	10	.970	.970	.000	.970	.000	.970	.000	.971	.001	.970	.000	.970	.000
2.23	25	.971	.972	.001	.971	.000	.971	.000	.971	.000	.971	.000	.971	.000
2.23	50	.972	.974	.002	.973	.001	.973	.001	.972	.000	.973	.001	.972	.000
2.23	80	.976	.976	.000	.976	.000	.975	.001	.977	.001	.975	.001	.977	.001
3.36	0	.955	.955	.000	.957	.002	.954	.001	.957	.002	.954	.001	.954	.001
3.36	10	.956	.957	.001	.957	.001	.955	.001	.958	.002	.955	.000	.955	.001
3.36	25	.957	.958	.001	.959	.002	.956	.001	.958	.001	.957	.001	.957	.001
3.36	50	.960	.961	.001	.961	.001	.959	.001	.961	.000	.960	.000	.960	.000
3.36	80	.964	.962	.002	.964	.000	.962	.002	.965	.001	.963	.001	.964	.000
6.67	0	.913	.917	.004	.919	.006	.914	.001	.918	.005	.914	.001	.913	.000
6.67	10	.916	.919	.003	.920	.004	.916	.000	.920	.004	.916	.000	.916	.000
6.67	25	.919	.921	.002	.922	.003	.918	.001	.922	.003	.919	.000	.919	.000
6.67	50	.924	.924	.000	.926	.002	.921	.003	.926	.002	.924	.000	.924	.000
6.67	80	.929	.929	.000	.930	.001	.926	.003	.930	.001	.929	.001	.928	.001
10.10	0	.878	.879	.001	.880	.002	.880	.002	.877	.001	.880	.002	.877	.000
10.10	10	.881	.882	.001	.882	.001	.882	.001	.881	.000	.882	.001	.881	.000
10.10	25	.885	.885	.000	.885	.000	.885	.000	.885	.000	.885	.000	.885	.000
10.10	50	.890	.890	.000	.889	.001	.889	.001	.891	.001	.889	.001	.890	.000
10.10	80	.893	.895	.002	.895	.002	.895	.002	.893	.000	.895	.002	.894	.001
11.74	0	.863	.862	.001	.860	.003	.865	.002	.857	.006	.865	.002	.862	.001
11.74	10	.866	.865	.001	.863	.003	.868	.002	.862	.004	.867	.001	.867	.001
11.74	25	.870	.869	.001	.866	.004	.871	.001	.867	.003	.870	.000	.870	.000
11.74	50	.874	.874	.000	.872	.002	.877	.003	.873	.001	.874	.000	.875	.001
11.74	80	.880	.880	.000	.879	.001	.883	.003	.876	.004	.880	.000	.878	.002

*   Nomograph of Figure 28
**   Equations from Table 6

(45)

range at higher salinities.

Where less accuracy can be tolerated, e.g., within about 1% of the experimental values, a very simple equation is useful:

$$C_p = 1.000 - 0.0125S + 0.00020T$$

where C_p is in calories/gram-°C, S is percent salinity, and T is °C.

The greatest deviation from experiment for this equation, for the 35 selected points of Table 7, is 0.013 calories; this occurs at the extremes of salinity: 0% and 11.7%.

NaCl Solutions

The differences between the heat capacity of sea water and of NaCl solutions are illustrated in Figure 29. The isothermal curves for sea water have been redrawn from Figure 27. The triangular points are those of the NaCl solutions. At increasing concentrations, the difference increases slightly; also, the temperature coefficient is less for the NaCl solution than for the sea water. No concentration frame of reference --weight percent (salinity), ionic strength, equal number of ions, or of ion equivalents --has been found for which the heat capacities of sea water parallel those of NaCl solutions across the entire concentration and temperature range.
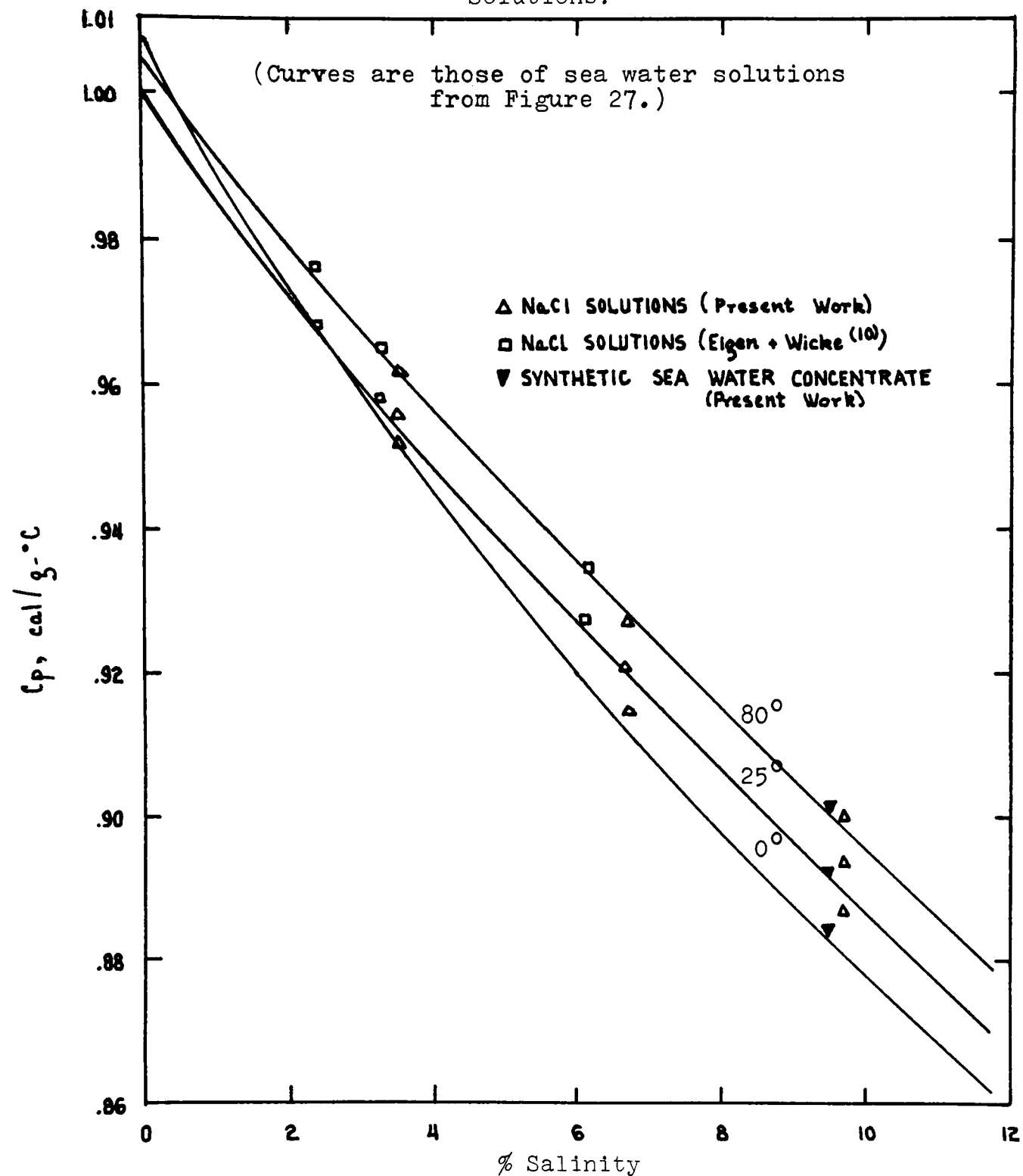
The square points in the figure are from data obtained by Eigen and Wicke[10] for NaCl solutions. They show excellent agreement with our data for the three concentrations included in their work. Unfortunately, their concentrations are not high enough to allow comparison for the triply concentrated sea water.

It may be concluded that where accuracies on the order of a few parts per thousand are required, NaCl solution data should not be substituted for sea water above concentrations twice that of natural sea water. Where an accuracy within about 1% suffices, the substitution may be made for heat capacities within the concentration range of 0-11.7% salinity and 2-80°C.

Synthetic Sea Water

The inverted triangles in Figure 29 refer to the synthetic sea water described on page 11. This reaffirms that agreement of natural sea water with synthetic sea water is better than it is with NaCl solutions. Figure 25 has shown some evidence that heat capacities of other

Figure 29   Comparison of Heat Capacities of NaCl
            Solutions with those of Sea Water
            Solutions.

(Curves are those of sea water solutions
              from Figure 27.)

△ NaCl SOLUTIONS (Present Work)
□ NaCl SOLUTIONS (Eigen + Wicke [10])
▼ SYNTHETIC SEA WATER CONCENTRATE
   (Present Work)

C_p, cal/g·°C

% Salinity

80°
25
0°

salts whose ions are present in sea water (in this case Na_2SO_4) have a stronger temperature dependence than NaCl solutions. A comparison in Table 9 of $MgCl_2$ and NaCl solution data of Eigen and Wicke[10] shows that the heat capacity of $MgCl_2$ solutions also have a much greater temperature dependence than NaCl solutions.

Table 9

COMPARISON OF TEMPERATURE DEPENDENCE OF HEAT CAPACITIES OF $MgCl_2$ AND NaCl SOLUTIONS
(Data from Eigen and Wicke[10])

Solution	$(C_p^{80°} - C_p^{10°})$, cal/g-°C
$MgCl_2$, 0.382 M	0.0089
NaCl, 0.405 M	0.0059
$MgCl_2$, 0.949 M	0.0156
NaCl, 1.120 M	0.0056

These differences among the effective heat capacities of ions increase with increasing concentration. Current research on other physical properties will seek to yield additional information on the effects of ions other than Na^+ and Cl^- on the behavior of sea water.

DESIGN AND CONSTRUCTION OF PRESSURE CALORIMETER

A major effort has been expended in the design, fabrication and assembly of a pressure calorimeter which will, when completed, extend our heat capacity measurements capability to 200°C.

The calorimeter was originally conceived as an adiabatic device which relied on a steam jacketed sample chamber to prevent heat flow to or from the sample. The design considered was found to involve difficulties in sample changing and required a very sophisticated temperature control system for the steam jacket.

Early in the year (1965), an isothermally jacketed calorimeter was considered as an alternate to the adiabatic device which would provide simpler design and operation. Calculations indicated that data of the desired accuracy could be obtained with an isothermal device, and consequently, this principle was adopted as a design criterion.

The isothermal device includes a dome shaped calorimeter bomb made of gold plated beryllium copper as shown upper center in Figure 30. Gold plating is required on the outside for minimizing radiant heat transfer, and on the inside for corrosion protection. The flat-plate closure is located just in front of the bomb; the stud attached to the closure is the support for the magnetic stirrer (the slave magnet). This disc-shaped magnet will be gold plated, and it will be mounted on a monel bearing. The design is such that monel vanes can be added to enhance the stirring action if required.

Beryllium copper was chosen as a high-strength bomb material to provide a low mass system which, at the same time, would have a high thermal conductance. These properties tend to reduce the heat capacity of the system, and the time lag of the calorimeter temperature; in both cases, the inherent accuracy of the apparatus is improved.

On the outside of the bomb are tapped bosses for attaching thermocouple assemblies, a valve for outgassing the sea water samples, and tapped holes to accept two resistance thermometers.

The heater, an example of which is shown in Figure 31, will rest on the closure plate of the bomb. It is made of two sections of well-mated copper tubing and is welded closed at either end. The inner tube has a bifilar thread on its outer surface; a fiber glass insulated resistance wire (10 mil ADVANCE alloy) fits snugly into this thread. The ends of the resistance wire are fused to 30 mil gold lead-out wires which are fed out through 1/8 inch copper tubes (see Figure 31) and insulated with thin teflon tubing. The ADVANCE resistance element is 40 feet long and has a heat output of about 100 watts at 100 volts. ADVANCE alloy was chosen because it has a very small temperature coefficient of resistance. The heater body is to be gold plated for corrosion resistance. Some preliminary tests indicate that a linear temperature response will be achieved in the calorimeter within about ten seconds after the power has been turned on. It has been estimated that the temperature rise of the resistance wire will be only 5 to 10°C during the heating cycle. A stable temperature drift is realized within one to two minutes after the power is turned off.

During experiments, the bomb will be contained in the oil-bath vacuum chamber shown in the oven (Figure 30). Silicone oil (Dow-Corning No. 210H) is to be circulated through an annular space between the inner and outer oil bath walls of the vacuum chamber. The oil will be controlled to ±0.001°C or better, and the oven temperature will be con-

Figure 30

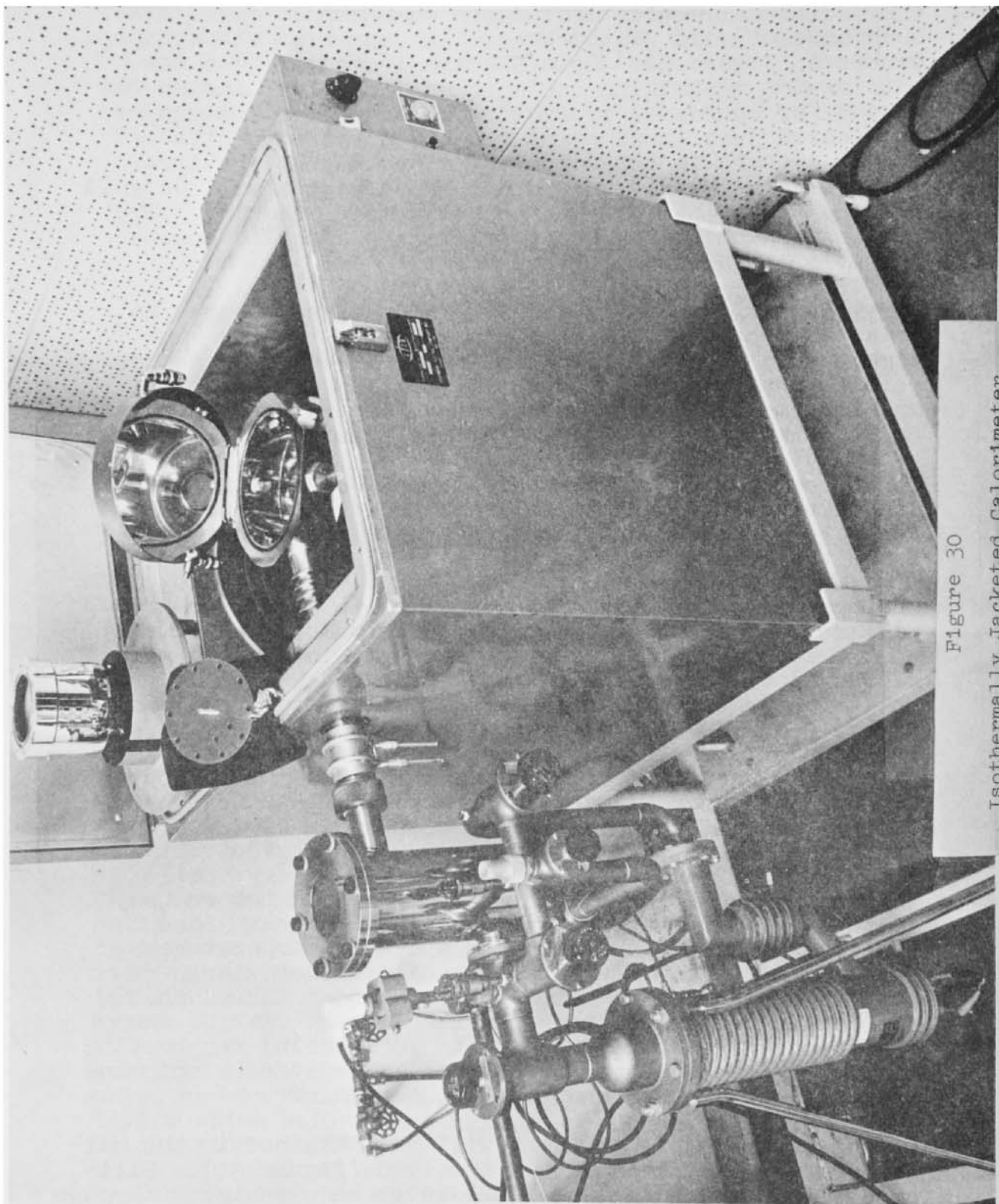Isothermally Jacketed Calorimeter

Figure 2

High Pressure Calorimeter Bomb

trolled to ±0.5°C or better. The inlet to outlet oil temperature difference has been estimated to be of the order of 0.0005°C.

The oil pump and the stirrer motor will be located under the oven; the diffusion pump and its dry-ice trap are shown to the left in Figure 30.

The calorimeter temperature will be recorded by a nickel-resistance thermometer-Bridge-Amplifier system. The recorded signal is the deviation from null, the sensitivity of which exceeds ±0.0001°C. The absolute temperature level will be determined by a platinum resistance thermometer-Mueller Bridge system. Tests indicate that drift temperatures can be satisfactorily recorded; drift rates of 0.017 and 0.05°C per hour have been estimated at 80 and 200°C respectively. Also, it has been determined that transient temperatures during heat-up can be recorded with our system and used to determine the effective "firing time" easily and accurately.

Other instrumentation, as shown in Figure 32, includes vacuum gauges; temperature controllers for the oven and oil bath, temperature indicators (for approximate values only) for the bomb, oil bath and oven; a solid state D.C. power supply; a heater-power safety cut out circuit; and a timing circuit.

The timing circuit is based on a standard pendulum clock. As conceived, electrical contact to close the heater relay would consist of a knife blade on the pendulum passing through a mercury bubble. Presently we are considering a photoelectric switching device.

The energy input is determined by measuring the voltage and current during an accurately determined time interval. To do this, a K-3 potentiometer will be used to measure the potential drop across appropriate standard resistors. The power supply is guaranteed to ±0.01% voltage stability.

In general, the design criterion has been 0.01% accuracy; we feel that an accuracy (overall) of ±0.1% should be readily obtainable.

The safety circuit is based on a commercial device which senses a thermocouple signal; if the thermocouple indicates a temperature exceeding 200°C, all heater power is cut out by a relay system.

Debugging of the apparatus, and heat capacity measurements will proceed under OSW Research Contract No. 14-01-0001-763.

Figure 32

High Pressure Calorimeter Instrumentation

List of References

1. R.A.Cox and N.D.Smith, Proc. Roy. Soc.(London) A 252, 51 (1959).

2. A.Weissberger, ed., Physical Methods of Organic Chemistry, 3rd Edition, Interscience Publishers, N. Y., Vol.1, Pt.1, p.530 (1959).

3. A.R.Challoner, H.A.Gundry, and A.R.Meetham, Phil. Trans. A 247, 553 (1955).

4. N.S.Osborne, H.F.Stimson, and D.C.Ginnings, J. Res. NBS 23, 238 (1939).

5. J.L.Reid, R.S.Arthur, and E.B.Bennett, eds., "Oceanic Observations of the Pacific", U. of California Press, Berkeley and Los Angeles, 1965.

6. "Data Report, Physical and Chemical Data, CCOFI Cruise 6401, January 10 to March 4, 1964", SIO Reference 65-7, April 5, 1965.

7. H.U.Sverdrup, M.W.Johnson, and R.H.Fleming, "The Oceans: their Physics, Chemistry, and General Biology", Prentice-Hall, Inc., Englewood Cliffs, N. J., 1942, p.50.

8. M.Randall and F.D.Rossini, J.Am.Chem.Soc. 51, 323 (1929).

9. C.B.Hess and B.E.Gramkee, J.Phys.Chem. 44, 483 (1940).

10. M.Eigen and E.Wicke, Z.Elektrochemie 55, 354 (1951).